Chapter 4
Numerical Solutions of Riesz Fractional Partial Differential Equations

4.1 Introduction

Nowadays, different applications of fractional differential equations in many areas, such as engineering, physics, chemistry, astrophysics, and many other sciences, are observed. Fractional kinetics systems are widely applied to describe anomalous diffusion or advection-dispersion processes [1]. Fractional differential equations are comprehensively used in examining physical phenomena in numerous disciplines of engineering and science. For this, we need reliable and efficient techniques for the solutions of fractional differential equations [2, 3]. The fractional-order models are more adequate than the previously used integer-order models because fractional-order derivatives and integrals enable the description of the memory and hereditary properties of different substances [4]. This is the most significant advantage of the fractional-order models in comparison with integer-order models, in which such effects are neglected. In the area of physics, fractional space derivatives are used to model anomalous diffusion or dispersion, where a particle spreads at a rate inconsistent with the classical Brownian motion model [5]. In particular, the Riesz fractional derivative includes a left Riemann–Liouville derivative and a right Riemann–Liouville derivative that allows the modeling of flow regime impacts from either side of the domain [6]. The fractional advection-dispersion equation (FADE) is used in groundwater hydrology to model the transport of passive tracers carried by fluid flow in a porous medium [7–9].

The Riesz fractional advection-dispersion equation (RFADE) with a symmetric fractional derivative, namely the Riesz fractional derivative, was derived from the kinetics of chaotic dynamics by Saichev and Zaslavsky [10] and summarized by Zaslavsky [6]. Ciesielski and Leszczynski [11] presented a numerical solution for the RFADE (without the advection term) based on the finite difference method. Shen et al. [12] presented explicit and implicit difference approximations for the space RFADE with initial and boundary conditions on a finite domain and derived the stability and convergence of their proposed numerical methods.

S. Saha Ray, *Nonlinear Differential Equations in Physics*,
https://doi.org/10.1007/978-981-15-1656-6_4

Fokker–Planck equation (FPE) was introduced by Adriaan Fokker and Max Planck, commonly used to describe the Brownian motion of particles [13]. The FPE describes the change of probability of a random function in space and time, so it is naturally used to describe solute transport. The FPE is involved with the conservation of probability that a particle will occupy a specific location. At any particular time, the sum of the probabilities at all locations must equal unity. So if the probability changes in one location from one moment to the next, the probability must also change in the vicinity to conserve probability. An ensemble of a large number of particles can fulfill the probabilities, and the FPE becomes an equation of the conservation of mass. Also, the nonlinear Fokker–Planck equation has important applications in various other fields. The fractional Fokker–Planck equations have been useful for the description of transport dynamics in complex systems that are governed by anomalous diffusion and nonexponential relaxation patterns [5]. Fractional derivatives play a key role in modeling particle transport in anomalous diffusion. For the description of anomalous transport in the presence of an external field, Metzler and Klafter [5] introduced a time fractional extension of the FPE, namely the time fractional Fokker–Planck equation (TFFPE).

There are some researchers who have investigated the FFPE. So and Liu [14] studied the subdiffusive fractional Fokker–Planck equation of bistable systems. Saha Ray and Gupta [15] established the numerical solutions of time and space fractional Fokker–Planck equations with the aid of two-dimensional Haar wavelets. Chen et al. [16] proposed three different implicit approximations for the TFFPE and proved these approximations are unconditionally stable and convergent. Zhuang et al. [17] presented an implicit numerical method for the TSFFPE and discussed its stability and convergence.

Numerous mathematical methods such as the Adomian decomposition method (ADM) [18], variational iteration method (VIM) [18], operational Tau method (OTM) [19], and homotopy perturbation method (HPM) [20] have been used in order to solve fractional Fokker–Planck equations. In Refs. [18–20], the fractional derivative is considered in Caputo sense. The aim of the present work is to implement shifted Grünwald approximation and fractional centered difference approximation to discretize the Riesz fractional diffusion equation and time and space Riesz fractional Fokker–Planck equation, respectively. The stability and convergence of the proposed finite difference schemes have been also analyzed rigorously.

The classical sine-Gordon equation (SGE) [21] is one of the basic equations of modern nonlinear wave theory, and it arises in many different areas of physics, such as nonlinear optics, Josephson junction theory, field theory, and the theory of lattices [22]. In these applications, the sine-Gordon equation provides the simplest nonlinear description of physical phenomena in different configurations. The theory, methods of solutions, and applications of the celebrated fractional sine-Gordon equation are discussed in great detail in two recent books [23, 24]. Special attention is also given to soliton, antisoliton solutions, and a remarkable new mode that propagates in a two-level atomic system. In order to further emphasis on the analysis of one-soliton and two-soliton solitary wave solutions, it may be referred to Ref. [25].

The more adequate modeling can be prevailed corresponding to the generalization of the classical sine-Gordon equation. In particular, taking into account of nonlocal effects, such as long-range interactions of particles, complex law of medium dispersion, or curvilinear geometry of the initial boundary problem, classical sine-Gordon equation results in the nonlocal generalization of SGE.

In this chapter, the nonlocal generalization of the sine-Gordon equation has been proposed in [26] as follows:

$$u_{tt} - {}^{R}D_{x}^{\alpha}u + \sin u = 0, \tag{4.1}$$

where the nonlocal operator ${}^{R}D_{x}^{\alpha}$ is the Riesz space fractional derivative, $1 \leq \alpha \leq 2$.

These similar types of evolution Eq. (4.2) arise in various interesting problems of nonlocal Josephson electrodynamics. These problems were introduced in [27–32]; among these, one of the basic model equation is

$$u_{tt} - H[u_x] + \sin u = 0, \tag{4.2}$$

where H is the Hilbert transform, given by

$$H[\phi] \equiv \frac{1}{\pi} v \cdot p \cdot \int_{-\infty}^{\infty} \frac{\phi(\xi)}{\xi - x} \mathrm{d}\xi, \tag{4.3}$$

and the integral is understood in the Cauchy principal value sense. The evolution Eq. (4.2) was an object of study in a series of papers [27, 28, 31, 33, 34] available in the open literature. Other nonlocal sine-Gordon equations were considered in [35, 36].

In this case, the derived approximate solutions are based on modified homotopy analysis method with Fourier transform. In this present chapter, we employ a new technique such as applying the Fourier transform followed by homotopy analysis method. This new technique enables derivation of the approximate solutions for the nonlocal fractional sine-Gordon Eq. (4.1). To the best possible information of the author, the present approximation technique has been proposed first time in this work for solving the nonlocal fractional sine-Gordon equation.

4.2 Outline of the Present Study

In this chapter, numerical solutions of fractional Fokker–Planck equations with Riesz space fractional derivatives have been developed. Here, the fractional Fokker–Planck equations have been considered in a finite domain. In order to deal with the Riesz fractional derivative operator, shifted Grünwald approximation and

fractional centered difference approaches have been used. The explicit finite difference method and Crank–Nicolson implicit method have been applied to obtain the numerical solutions of the fractional diffusion equation and fractional Fokker–Planck equations, respectively. Numerical results are presented to demonstrate the accuracy and effectiveness of the proposed numerical solution techniques.

Also, a novel approach comprising modified homotopy analysis method with Fourier transform has been implemented for the approximate solution of the fractional sine-Gordon equation

$$u_{tt} - {}^{R}D_{x}^{\alpha}u + \sin u = 0,$$

where ${}^{R}D_{x}^{\alpha}$ is the Riesz space fractional derivative, $1 \leq \alpha \leq 2$.

For $\alpha = 2$, it becomes a classical sine-Gordon equation

$$u_{tt} - u_{xx} + \sin u = 0,$$

and corresponding to $\alpha = 1$, it becomes nonlocal sine-Gordon equation

$$u_{tt} - Hu + \sin u = 0,$$

which arises in Josephson junction theory, where H is the Hilbert transform. The fractional sine-Gordon equation is considered as an interpolation between the classical sine-Gordon equation (corresponding to $\alpha = 2$) and nonlocal sine-Gordon equation (corresponding to $\alpha = 1$). Here the approximate solution of the fractional sine-Gordon equation is derived by using the modified homotopy analysis method with Fourier transform. Then, the obtained results have been analyzed by numerical simulations, which demonstrate the simplicity and effectiveness of the present method.

4.3 Numerical Approximation Techniques for Riesz Space Fractional Derivative

There are different approximation techniques for Riesz space fractional derivative [37–40]. In the present chapter, the emphasis has been focused on the shifted Grünwald formula to discretize the Riesz space fractional differential equation which, unlike the standard Grünwald formula, does not suffer from instability problems [41] and also on the fractional centered difference approximation technique, respectively.

Let us assume that the function $W(x,t)$ is $n-1$ times continuously differentiable in the interval $[0,L]$ and that $W^{(n)}(x,t)$ is integrable in $[0,L]$. Then for every $\alpha(0 \leq n-1 < \alpha \leq n, n \in \mathbf{N})$, the Riemann–Liouville fractional derivative exists and coincides with the Grünwald–Letnikov derivative. This relationship enables the use of the Grünwald–Letnikov derivative for obtaining the numerical solution [8, 42].

The fractional Grünwald–Letnikov derivative with order $1-\alpha$ is given by

$$\begin{aligned} {}_0D_t^{1-\alpha}W(x,t_k) &= \lim_{\tau\to 0}\tau^{\alpha-1}\sum_{r=0}^{k}(-1)^r\binom{1-\alpha}{r}W(x,t_k-r\tau) \\ &= \tau^{\alpha-1}\sum_{r=0}^{k}\omega_r^{1-\alpha}W(x,t_k-r\tau)+O(\tau^p), \end{aligned} \tag{4.4}$$

where $\tau = T/N$, $t_r = r\tau$, $\omega_0^{1-\alpha} = 1$, $\omega_r^{1-\alpha} = (-1)^r\frac{(1-\alpha)(-\alpha)\ldots(2-\alpha-r)}{r!}$, for $r = 1, 2\ldots, N$.

4.3.1 Shifted Grünwald Approximation Technique for the Riesz Space Fractional Derivative

The shifted Grünwald formula which was proposed by Meerschaert and Tadjeran [41] has been applied for discretizing the Riesz fractional derivative. In this problem, we discretize the Riesz space fractional derivative using the following shifted Grünwald approximation:

$$\frac{\partial^\alpha W(x_l,t)}{\partial|x|^\alpha} \approx -\frac{h^{-\alpha}}{2\cos\left(\frac{\alpha\pi}{2}\right)}\left[\sum_{j=0}^{l+1}\tilde{g}_j W_{l-j+1}+\sum_{j=0}^{m-l+1}\tilde{g}_j W_{l+j-1}\right], \tag{4.5}$$

where the coefficients are defined by

$$\tilde{g}_0 = 1, \tilde{g}_j = (-1)^j\frac{\alpha(\alpha-1)\ldots(\alpha-j+1)}{j!}, \quad j = 1,2,\ldots,m.$$

4.3.2 Fractional Centered Difference Approximation Technique for the Riesz Space Fractional Derivative

Recently, Çelik and Duman [43] derived the interesting result that if $f^*(x)$ be defined as follows

$$f^*(x) = \begin{cases} f(x), & x\in[a,b] \\ 0, & x\notin[a,b] \end{cases}$$

such that $f^*(x)\in C^5(\mathsf{R})$ and all derivatives up to order five belong to $L_1(\mathsf{R})$, then for the Riesz fractional derivative of order $\alpha(1<\alpha\le 2)$

$$\frac{\partial^{\alpha} f(x)}{\partial |x|^{\alpha}} = -h^{-\alpha} \sum_{j=-\frac{b-x}{h}}^{\frac{x-a}{h}} g_j f(x - jh) + O(h^2), \tag{4.6}$$

where $h = \frac{b-a}{m}$, and m is the number of partitions of the interval $[a, b]$ and

$$g_j = \frac{(-1)^j \Gamma(\alpha + 1)}{\Gamma(\alpha/2 - j + 1)\Gamma(\alpha/2 + j + 1)}.$$

Property 4.1 *The coefficients g_j of the fractional centered difference approximation have the following properties for $j = 0, \mp 1, \mp 2, \ldots$, and $\alpha > -1$:*

(i) $g_0 \geq 0$,
(ii) $g_{-j} = g_j \leq 0$ *for all* $|j| \geq 1$,
(iii) $g_{j+1} = \frac{j - \alpha/2}{\alpha/2 + j + 1} g_j$,
(iv) $g_j = O(j^{-\alpha - 1})$.

Proof For the proof of the above properties, it may be referred to Ref. [43].

Lemma 4.1 *Let $f \in C^5(\mathsf{R})$ and all derivatives up to order five belong to $L_1(\mathsf{R})$ and the fractional central derivative of f be*

$$\delta^{\alpha} f(x) = \sum_{j=-\infty}^{\infty} g_j f(x - jh),$$

where

$$g_j = \frac{(-1)^j \Gamma(\alpha + 1)}{\Gamma(\alpha/2 - j + 1)\Gamma(\alpha/2 + j + 1)},$$

then

$$\frac{\partial^{\alpha} f(x)}{\partial |x|^{\alpha}} = -h^{-\alpha} \sum_{j=-\infty}^{\infty} g_j f(x - jh) + O(h^2),$$

when $h \to 0$ and $\frac{\partial^{\alpha} f(x)}{\partial |x|^{\alpha}}$ is the Riesz fractional derivative for $1 < \alpha \leq 2$.

Proof For the proof also, it may be referred to Ref. [43].

4.3.3 Inhomogeneous Fractional Diffusion Equation with Riesz Space Fractional Derivative

Let us consider the following inhomogeneous Riesz fractional diffusion equation with source term in a finite domain associated with initial and Dirichlet boundary conditions [42, 43]

$$\frac{\partial W(x,t)}{\partial t} = K\frac{\partial^{\alpha} W(x,t)}{\partial |x|^{\alpha}} + f(x,t), a < x < b, \quad t \in [0,T], \tag{4.7}$$

$$W(x,0) = \phi(x), a \le x \le b,$$
$$W(a,t) = W(b,t) = 0, 0 \le t \le T,$$

where $K > 0$ is diffusion coefficient and $\phi(x)$ is a real-valued sufficiently smooth function. We consider a super-diffusion model, i.e., $1 < \alpha \le 2$. This type of super-diffusion problems largely arises in the modeling of fluid flow, finance, and other applications.

Explicit Finite Difference Method for Riesz Fractional Diffusion Equation

In this present analysis, numerical solution of Eq. (4.7) has been provided based on the explicit finite difference method (EFDM). Let us assume that the spatial domain is $[0, L]$, and it is partitioned into m subintervals. Thus, the mesh is of m equal subintervals of width $h = L/m$ and $x_l = lh$, for $l = 0, 1, 2, \ldots, m$. Let W_l^k denote the numerical approximation of $W(x_l, t_k)$ at (x_l, t_k).

Now we obtain the following explicit finite difference numerical discretization scheme for the Eq. (4.7).

$$W_l^{k+1} = W_l^k + \tau\left[-\frac{Kh^{-\alpha}}{2\cos\left(\frac{\alpha\pi}{2}\right)}\left(\sum_{j=0}^{l+1}\tilde{g}_j W_{l-j+1}^k + \sum_{j=0}^{m-l+1}\tilde{g}_j W_{l+j-1}^k\right) + f_l^k\right], \tag{4.8}$$

for $l = 1, 2, \ldots, m-1$, and $k = 0, 1, \ldots, N-1$.

The aforementioned Eq. (4.8) determines the numerical approximate value of the solution W_l^{k+1} at (x_l, t_{k+1}).

In matrix form, Eq. (4.8) can be written as

$$\boldsymbol{U}^{k+1} = \boldsymbol{A}\boldsymbol{U}^k + \tau \boldsymbol{F}^{k+1/2}, \tag{4.9}$$

where $\boldsymbol{U}^k = (W_1^k, W_2^k, \ldots, W_{m-1}^k)^T$,

$\boldsymbol{F}^k = \left[f_1^k, f_2^k, \ldots, f_{m-1}^k\right]^T$, and $\boldsymbol{A}_i$ is a symmetric $(m-1)\times(m-1)$ matrix of the following form

$$\boldsymbol{A} = \begin{pmatrix} 1 - \frac{K\tau h^{-\alpha}}{\cos\frac{\alpha\pi}{2}}\tilde{g}_1 & -\frac{K\tau h^{-\alpha}}{2\cos\frac{\alpha\pi}{2}}(\tilde{g}_0+\tilde{g}_2) & -\frac{K\tau h^{-\alpha}}{2\cos\frac{\alpha\pi}{2}}\tilde{g}_3 & \cdots & -\frac{K\tau h^{-\alpha}}{2\cos\frac{\alpha\pi}{2}}\tilde{g}_{m-1} \\ -\frac{K\tau h^{-\alpha}}{2\cos\frac{\alpha\pi}{2}}(\tilde{g}_0+\tilde{g}_2) & 1 - \frac{K\tau h^{-\alpha}}{\cos\frac{\alpha\pi}{2}}\tilde{g}_1 & -\frac{K\tau h^{-\alpha}}{2\cos\frac{\alpha\pi}{2}}(\tilde{g}_0+\tilde{g}_2) & \cdots & -\frac{K\tau h^{-\alpha}}{2\cos\frac{\alpha\pi}{2}}\tilde{g}_{m-2} \\ \cdots & \cdots & \cdots & \cdots & \\ -\frac{K\tau h^{-\alpha}}{2\cos\frac{\alpha\pi}{2}}\tilde{g}_{m-1} & -\frac{K\tau h^{-\alpha}}{2\cos\frac{\alpha\pi}{2}}\tilde{g}_{m-2} & -\frac{K\tau h^{-\alpha}}{2\cos\frac{\alpha\pi}{2}}\tilde{g}_{m-3} & \cdots & 1 - \frac{K\tau h^{-\alpha}}{\cos\frac{\alpha\pi}{2}}\tilde{g}_1 \end{pmatrix}. \tag{4.10}$$

4.3.4 Time and Space Fractional Fokker–Planck Equation with Riesz Fractional Operator

In this section, we consider the following time and space fractional Fokker–Planck equation which describes the anomalous transport in the presence of an external field [42]

$$\frac{\partial W(x,t)}{\partial t} = {}_0D_t^{1-\alpha}\left[\left(\frac{\partial}{\partial x}\frac{V'(x)}{m\eta_\alpha} + K_\alpha^\mu \frac{\partial^\mu}{\partial|x|^\mu}\right)W(x,t) + f(x,t)\right], a < x < b, \quad t \in [0,T], \tag{4.11}$$

subject to initial and homogeneous Dirichlet boundary conditions

$$W(x,0) = \phi(x), a \le x \le b,$$
$$W(a,t) = W(b,t) = 0, 0 \le t \le T,$$

where K_α^μ denotes the anomalous diffusion coefficient; m is the mass of the diffusing test particle; η_α is the generalized friction constant of dimension $[\eta_\alpha] = s^{\alpha-2}$; $\frac{V'(x)}{m\eta_\alpha}$ is known as the drift coefficient, and the force is related to the external potential through $F(x) = -\frac{\mathrm{d}V(x)}{\mathrm{d}x}$. ${}_0D_t^{1-\alpha}(.)$ denotes the Riemann–Liouville time fractional derivative of order $1-\alpha(0<\alpha<1)$ defined by [44–47]

$${}_0D_t^{1-\alpha}\psi(x,t) = \frac{1}{\Gamma(\alpha)}\frac{\partial}{\partial t}\int_0^t \frac{\psi(x,\zeta)}{(t-\zeta)^{1-\alpha}}\mathrm{d}\zeta. \tag{4.12}$$

For $\alpha \to 1$ and $\mu \to 2$, the standard Fokker–Planck equation [5] is recovered, and for $\alpha \to 1$ and $V(x) \equiv$ const., i.e., in the force-free limit, the inhomogeneous fractional diffusion Eq. (4.7) emerges.

The Riesz space fractional derivative of order $v(1<v<2)$ is defined by [48, 49]

$$\frac{\partial^v W(x_l,t)}{\partial|x|^v} = -\frac{1}{2\cos\left(\frac{\pi v}{2}\right)}\left({}_aD_x^v + {}_xD_b^v\right)W(x,t), \tag{4.13}$$

where ${}_aD_x^v$ and ${}_xD_b^v$ are the left and right Riemann–Liouville space fractional derivative operators of order v, which are, respectively, given by

$${}_aD_x^v W(x,t) = \frac{1}{\Gamma(2-v)}\frac{\partial^2}{\partial x^2}\int_a^x \frac{W(\xi,t)}{(x-\xi)^{v-1}}\mathrm{d}\xi,$$

$${}_xD_b^v W(x,t) = \frac{1}{\Gamma(2-v)}\frac{\partial^2}{\partial x^2}\int_x^b \frac{W(\xi,t)}{(\xi-x)^{v-1}}\mathrm{d}\xi.$$

Implicit Finite Difference Method for Time and Riesz Space Fractional Fokker–Planck Equation

In order to solve Eq. (4.11) with the drift coefficient $-v$, fractional centered difference approximation along with Grünwald–Letnikov derivative approximation has been used to discretize it.

From Taylor's theorem, we have

$$\frac{W_l^{k+1}-W_l^k}{\tau} = \left(\frac{\partial W}{\partial t}\right)_l^{k+1/2} + O(\tau^2), \tag{4.14}$$

where the central difference with step size $\tau/2$ has been used.

Thus, using Eq. (4.14) and Lemma 4.1, we obtain the following implicit finite difference discretization scheme

$$\begin{aligned}\frac{W_l^{k+1}-W_l^k}{\tau} = \frac{1}{2}\Bigg[&-v\tau^{\alpha-1}\sum_{j=0}^{k}\omega_j^{1-\alpha}\left(\frac{W_{l+1}^{k-j}-W_l^{k-j}}{h}\right)\\ &-K_\alpha^\mu\,\tau^{\alpha-1}\,h^{-\mu}\sum_{j=0}^{k}\omega_j^{1-\alpha}\sum_{i=l-m}^{l}g_i W_{l-i}^{k-j}+\tau^{\alpha-1}\sum_{j=0}^{k}\omega_j^{1-\alpha}f_l^{k-j}\\ &-v\tau^{\alpha-1}\sum_{j=0}^{k+1}\omega_j^{1-\alpha}\left(\frac{W_{l+1}^{k+1-j}-W_l^{k+1-j}}{h}\right)-K_\alpha^\mu\,\tau^{\alpha-1}\,h^{-\mu}\sum_{j=0}^{k+1}\omega_j^{1-\alpha}\sum_{i=l-m}^{l}g_i W_{l-i}^{k+1-j}\\ &+\tau^{\alpha-1}\sum_{j=0}^{k+1}\omega_j^{1-\alpha}f_l^{k+1-j}\Bigg]+TE_l^{k+1/2},\end{aligned} \tag{4.15}$$

for $l=1,2,\ldots,m-1$, and $k=0,1,\ldots,N-1$, where the local truncation error $TE_l^{k+1/2}\equiv O(\tau^2+h^2)$.

Now, omitting the local truncation error in Eq. (4.15), we obtain

$$
\begin{aligned}
&W_l^{k+1}+\frac{v\tau^\alpha}{2}\omega_0^{1-\alpha}\left(\frac{W_{l+1}^{k+1}-W_l^{k+1}}{h}\right)+K_\alpha^\mu\frac{\tau^\alpha}{2}h^{-\mu}\omega_0^{1-\alpha}\sum_{i=l-m}^{l}g_iW_{l-i}^{k+1}=W_l^k\\
&-\frac{v\tau^\alpha}{2}\sum_{r=0}^{k}\omega_r^{1-\alpha}\left(\frac{W_{l+1}^{k-r}-W_l^{k-r}}{h}\right)-K_\alpha^\mu\frac{\tau^\alpha}{2}h^{-\mu}\sum_{r=0}^{k}\omega_r^{1-\alpha}\sum_{i=l-m}^{l}g_iW_{l-i}^{k-r}\\
&+\frac{\tau^\alpha}{2}\left(\sum_{r=0}^{k}\omega_r^{1-\alpha}f_l^{k-r}+\sum_{r=0}^{k+1}\omega_r^{1-\alpha}f_l^{k+1-r}\right)-v\frac{\tau^\alpha}{2}\sum_{r=1}^{k+1}\omega_r^{1-\alpha}\left(\frac{W_{l+1}^{k+1-r}-W_l^{k+1-r}}{h}\right)\\
&-K_\alpha^\mu\frac{\tau^\alpha}{2}h^{-\mu}\sum_{r=1}^{k+1}\omega_r^{1-\alpha}\sum_{i=l-m}^{l}g_iW_{l-i}^{k+1-r}.
\end{aligned}
\tag{4.16}
$$

Further, Eq. (4.16) can be written into the following matrix form

$$
\begin{aligned}
(\boldsymbol{I}+\boldsymbol{A}_0)\boldsymbol{U}^{k+1}=&(\boldsymbol{I}-\boldsymbol{A}_0-\boldsymbol{A}_1)\boldsymbol{U}^k-(\boldsymbol{A}_1+\boldsymbol{A}_2)\boldsymbol{U}^{k-1}-(\boldsymbol{A}_2+\boldsymbol{A}_3)\boldsymbol{U}^{k-2}-\cdots\\
&-(\boldsymbol{A}_k+\boldsymbol{A}_{k+1})\boldsymbol{U}^0+\tau^\alpha\boldsymbol{F}^{k+1/2},
\end{aligned}
\tag{4.17}
$$

where $\boldsymbol{U}^k=(W_1^k,W_2^k,\ldots,W_{m-1}^k)^T$,

$$
\begin{aligned}
F^{k+1/2}=&\left[\frac{1}{2}\left(\sum_{r=0}^{k}\omega_r^{1-\alpha}f_1^{k-r}+\sum_{r=0}^{k+1}\omega_r^{1-\alpha}f_1^{k+1-r}\right),\frac{1}{2}\left(\sum_{r=0}^{k}\omega_r^{1-\alpha}f_2^{k-r}+\sum_{r=0}^{k+1}\omega_r^{1-\alpha}f_2^{k+1-r}\right),\right.\\
&\left.\ldots,\frac{\tau^\alpha}{2}\left(\sum_{r=0}^{k}\omega_r^{1-\alpha}f_{m-1}^{k-r}+\sum_{r=0}^{k+1}\omega_r^{1-\alpha}f_{m-1}^{k+1-r}\right)\right]^T,
\end{aligned}
$$

and $\boldsymbol{A}_i$ is an $(m-1)\times(m-1)$ matrix of the following form

$$
\boldsymbol{A}_i=\omega_i^{1-\alpha}\begin{pmatrix}
-\frac{v\tau^\alpha}{2h}+\frac{K_\alpha^\mu\tau^\alpha}{2}h^{-\mu}g_0 & \frac{v\tau^\alpha}{2h}+\frac{K_\alpha^\mu\tau^\alpha}{2}h^{-\mu}g_{-1} & \cdots & \frac{K_\alpha^\mu\tau^\alpha}{2}h^{-\mu}g_{2-m}\\
\frac{K_\alpha^\mu\tau^\alpha}{2}h^{-\mu}g_1 & -\frac{v\tau^\alpha}{2h}+\frac{K_\alpha^\mu\tau^\alpha}{2}h^{-\mu}g_0 & \cdots & \frac{K_\alpha^\mu\tau^\alpha}{2}h^{-\mu}g_{3-m}\\
\cdots & \cdots & \cdots & \cdots\\
\frac{K_\alpha^\mu\tau^\alpha}{2}h^{-\mu}g_{m-2} & \frac{K_\alpha^\mu\tau^\alpha}{2}h^{-\mu}g_{m-3} & \cdots & -\frac{v\tau^\alpha}{2h}+\frac{K_\alpha^\mu\tau^\alpha}{2}h^{-\mu}g_0
\end{pmatrix}.
\tag{4.18}
$$

Now, we define the function space as follows: $\Lambda(\Omega)=\left\{W(x,t)\middle|\frac{\partial^5W(x,t)}{\partial x^5},\frac{\partial^4W(x,t)}{\partial x^2\partial t^2}\in C(\Omega)\right\}$, where $\Omega\equiv[a,b]\times[0,T]$. In this work, we assume that the Problems (4.7) and (4.11) have a smooth exact solution $W(x,t)\in\Lambda(\Omega)$, and $f(x,t)$ and $\phi(x)$ are sufficiently smooth functions.

4.3.5 Numerical Results for Riesz Fractional Diffusion Equation and Riesz Fractional Fokker–Planck Equation

In the present section, the numerical examples for Riesz fractional diffusion Eq. (4.7) and time and Riesz space fractional Fokker–Planck Eq. (4.11) with the drift coefficient $-v$ have been presented to demonstrate the effectiveness of the above-discussed numerical schemes for solving Riesz fractional diffusion equation and time-space fractional Fokker–Planck equation with Riesz derivative operator.

Example 4.1 Let us consider the following Riesz fractional diffusion equation [42, 43] on the finite domain $[0, 1]$.

$$\frac{\partial W(x,t)}{\partial t} = K\frac{\partial^{\alpha} W(x,t)}{\partial |x|^{\alpha}} + f(x,t), 0 < x < 1, \quad t \in [0,T], \tag{4.19}$$

subject to initial and homogeneous Dirichlet boundary conditions

$$W(x,0) = x^2(1-x)^2, 0 \le x \le 1,$$
$$W(0,t) = W(1,t) = 0, 0 \le t \le T$$

and the nonhomogenous part is

$$f(x,t) = (1+t)^{-1+\alpha}(-1+x)^2x^2\alpha + \frac{1}{\Gamma(5-\alpha)}x^{-\alpha}\left[\left(\frac{1+t}{1-x}\right)^{\alpha}(-1+x)^2x^{\alpha}(12x^2 - 6x\alpha + (-1+\alpha)\alpha) + (1+t)^{\alpha}x^2\left[12(-1+x)^2 + (-7+6x)\alpha + \alpha^2\right]\right]\sec\left(\frac{\pi\alpha}{2}\right).$$

The exact solution is

$$W(x,t) = (1+t)^{\alpha}x^2(1-x)^2. \tag{4.20}$$

In this example, we take $K = 1$, $\tau = 0.001$, and $h = 0.05$. Figures 4.1, 4.2, and 4.3 show the comparison of the exact and numerical solutions when $\alpha = 1.5$ at $t = 1, 3, 5$, respectively. It can be easily observed that the numerical solutions are in good agreement with the exact solution.

Example 4.2 Let us consider the following time fractional Fokker–Planck equation with Riesz space fractional derivative operator [42]

$$\frac{\partial W(x,t)}{\partial t} = {}_0D_t^{1-\alpha}\left[\left(-v\frac{\partial}{\partial x} + K_{\alpha}^{\mu}\frac{\partial^{\mu}}{\partial |x|^{\mu}}\right)W(x,t) + f(x,t)\right], 0 < x < 1, \quad t \in [0,T], \tag{4.21}$$

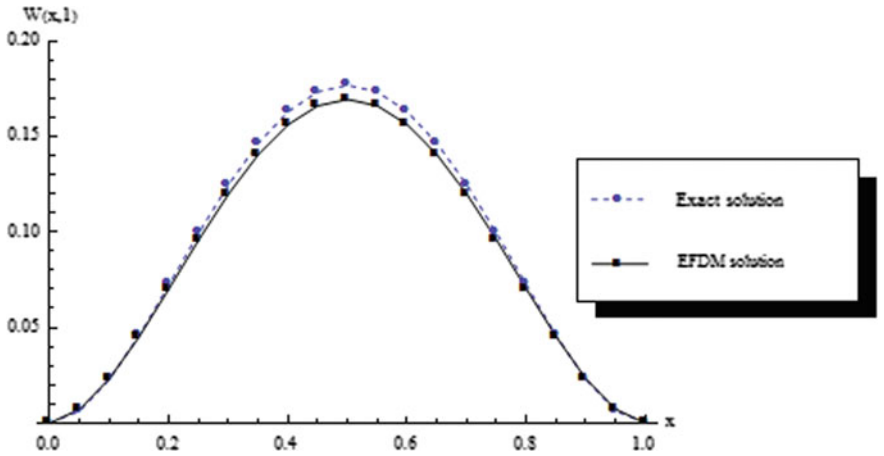

Fig. 4.1 Comparison of numerical solution of $W(x,t)$ with the exact solution at $t = 1$ for Example 4.1 with $\alpha = 1.5$, $h = 0.05$, and $\tau = 0.001$

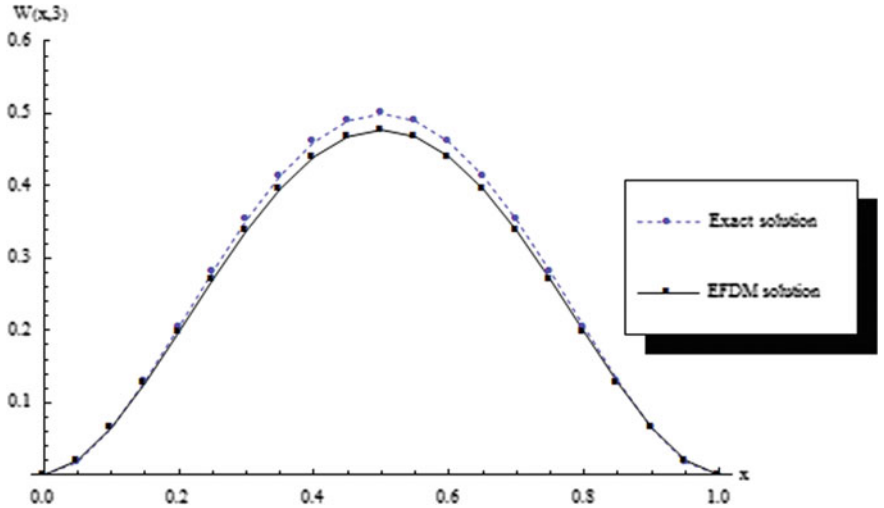

Fig. 4.2 Comparison of numerical solution of $W(x,t)$ with the exact solution at $t = 3$ for Example 4.1 with $\alpha = 1.5$, $h = 0.05$, and $\tau = 0.001$

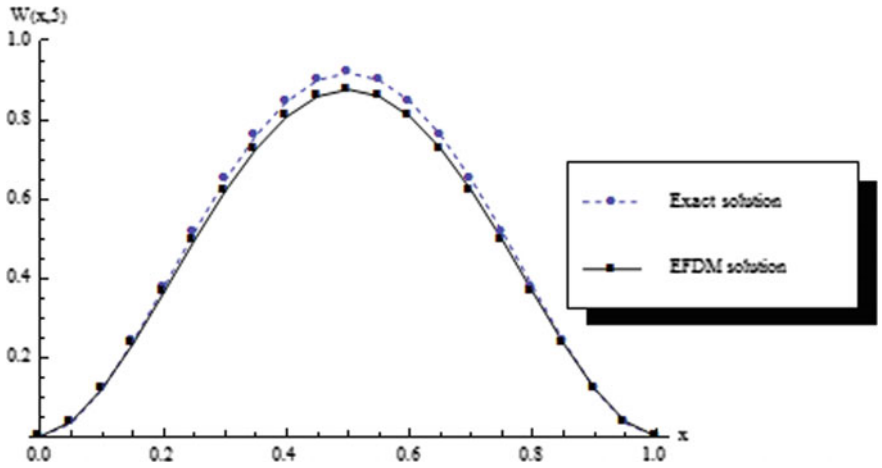

Fig. 4.3 Comparison of numerical solution of $W(x,t)$ with the exact solution at $t = 5$ for Example 4.1 with $\alpha = 1.5$, $h = 0.05$, and $\tau = 0.001$

subject to initial and homogeneous Dirichlet boundary conditions

$$W(x,0) = K_\alpha^\mu x^2(1-x)^2, 0 \le x \le 1,$$
$$W(0,t) = W(1,t) = 0, 0 \le t \le T,$$

The exact solution is

$$W(x,t) = (K_\alpha^\mu + vt^{1+\alpha})x^2(1-x)^2. \tag{4.22}$$

In this example, we take $K_\alpha^\mu = 25$, $\tau = 0.001$, $h = 0.05$, $\alpha = 0.8$, and $\mu = 1.9$. Figure 4.4 shows the comparison between the exact and numerical solutions at $t = 1$. In Fig. 4.5, comparison of numerical solution of $W(x,t)$ with the exact solution at $t = 3$ has been presented for Example 4.2 with $\alpha = 0.8$, $\mu = 1.9$, $h = 0.02$, and $\tau = 0.075$. Figure 4.6 explores the comparison of results for Example 4.2 with $\alpha = 0.8$, $\mu = 1.9$, $h = 0.02$, and $\tau = 0.1$. It can be clearly observed from the presented figures that the implicit finite difference solutions highly agree with the exact solutions.

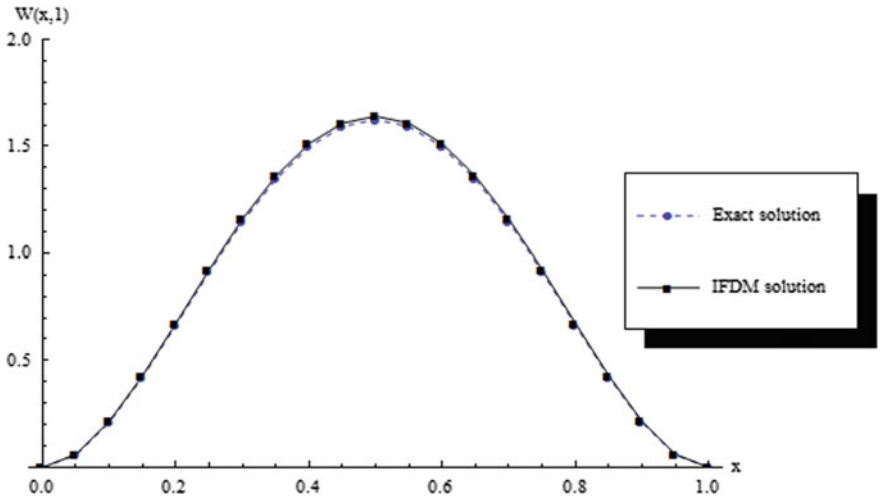

Fig. 4.4 Comparison of numerical solution of $W(x,t)$ with the exact solution at $t=1$ for Example 4.2 with $\alpha=0.8$, $\mu=1.9$, $h=0.05$, and $\tau=0.01$

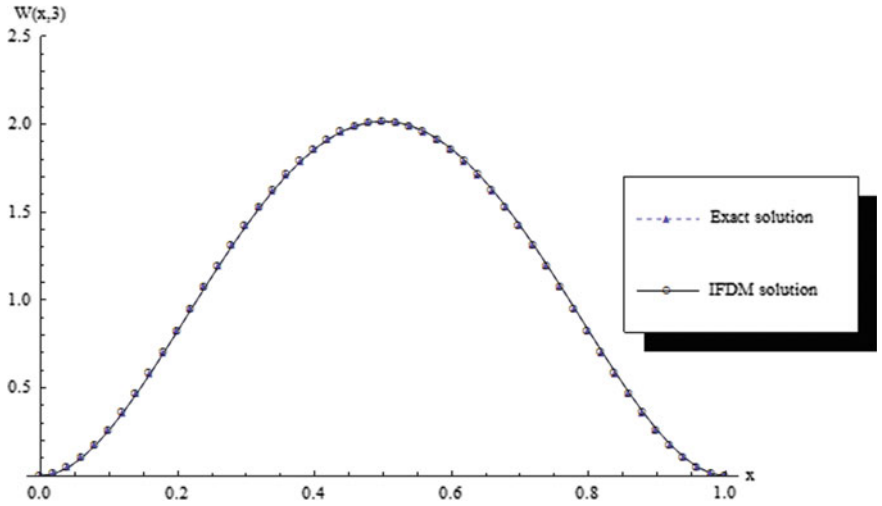

Fig. 4.5 Comparison of numerical solution of $W(x,t)$ with the exact solution at $t=3$ for Example 4.2 with $\alpha=0.8$, $\mu=1.9$, $h=0.02$, and $\tau=0.075$

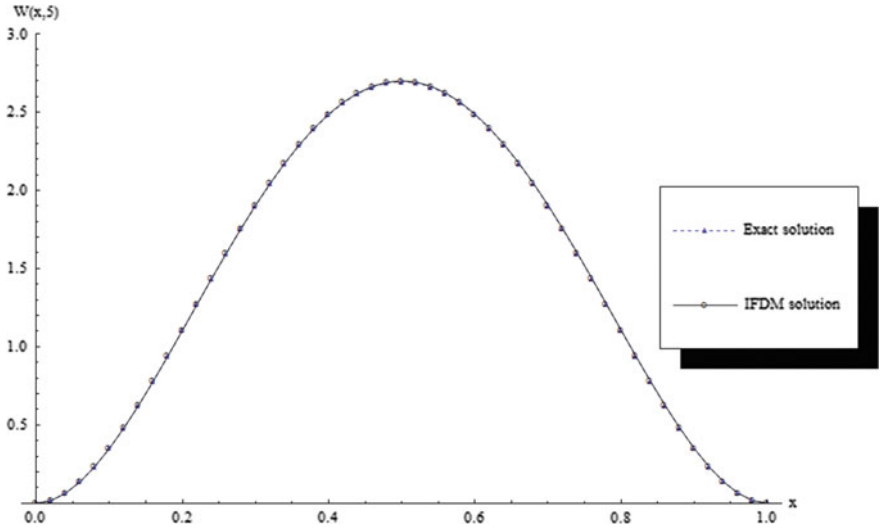

Fig. 4.6 Comparison of numerical solution of $W(x,t)$ with the exact solution at $t=5$ for Example 4.2 with $\alpha=0.8$, $\mu=1.9$, $h=0.02$, and $\tau=0.1$

4.3.6 *Stability and Convergence of the Proposed Finite Difference Schemes*

Theorem 4.1 *The numerical discretization scheme for the problem in* Eq. (4.19) *is stable, if*

$$r=\frac{\tau}{h^{\alpha}}\leq\frac{2\left|\cos\frac{\alpha\pi}{2}\right|}{K\left(\frac{\tilde{g}_1-(\tilde{g}_0+\tilde{g}_2)}{\operatorname{sgn}\left(\cos\frac{\alpha\pi}{2}\right)}+\tilde{g}_0\right)},\quad \text{for } 1<\alpha\leq 2.$$

Proof The matrix A in Eq. (4.10) can be written as

$$A=T+R, \tag{4.23}$$

where T is a tridiagonal $(m-1)\times(m-1)$ matrix of the following form

$$T=\begin{pmatrix} 1-\frac{K\tau h^{-\alpha}}{\cos\frac{\alpha\pi}{2}}\tilde{g}_1 & -\frac{K\tau h^{-\alpha}}{2\cos\frac{\alpha\pi}{2}}(\tilde{g}_0+\tilde{g}_2) & 0 & \dots & 0 \\ -\frac{K\tau h^{-\alpha}}{2\cos\frac{\alpha\pi}{2}}(\tilde{g}_0+\tilde{g}_2) & 1-\frac{K\tau h^{-\alpha}}{\cos\frac{\alpha\pi}{2}}\tilde{g}_1 & -\frac{K\tau h^{-\alpha}}{2\cos\frac{\alpha\pi}{2}}(\tilde{g}_0+\tilde{g}_2) & \dots & 0 \\ \dots & \dots & \dots & \dots & \dots \\ 0 & 0 & 0 & \dots & 1-\frac{K\tau h^{-\alpha}}{\cos\frac{\alpha\pi}{2}}\tilde{g}_1 \end{pmatrix}, \tag{4.24}$$

and R is a symmetric $(m-1)\times(m-1)$ matrix of the following form

$$R=\begin{pmatrix} 0 & 0 & -\frac{K\tau h^{-\alpha}}{2\cos\frac{\alpha\pi}{2}}\tilde{g}_3 & \cdots & -\frac{K\tau h^{-\alpha}}{2\cos\frac{\alpha\pi}{2}}\tilde{g}_{m-1} \\ 0 & 0 & 0 & \cdots & -\frac{K\tau h^{-\alpha}}{2\cos\frac{\alpha\pi}{2}}\tilde{g}_{m-2} \\ \cdots & \cdots & \cdots & \cdots & \cdots \\ -\frac{K\tau h^{-\alpha}}{2\cos\frac{\alpha\pi}{2}}\tilde{g}_{m-1} & -\frac{K\tau h^{-\alpha}}{2\cos\frac{\alpha\pi}{2}}\tilde{g}_{m-2} & -\frac{K\tau h^{-\alpha}}{2\cos\frac{\alpha\pi}{2}}\tilde{g}_{m-3} & \cdots & 0 \end{pmatrix}.$$

Now, let λ_i be the eigenvalue of the matrix R. Then, according to the Gerschgorin circle theorem [50], we have

$$|\lambda_i-0|\le\frac{K\tau h^{-\alpha}}{2\left|\cos\frac{\alpha\pi}{2}\right|}\sum_{k=3}^{m-1}|\tilde{g}_k|<\frac{K\tau h^{-\alpha}}{2\left|\cos\frac{\alpha\pi}{2}\right|}\sum_{k=3}^{\infty}\tilde{g}_k<\frac{K\tau h^{-\alpha}}{2\left|\cos\frac{\alpha\pi}{2}\right|}, \tag{4.25}$$

where $\sum_{k=3}^{\infty}\tilde{g}_k=-1+\alpha-\frac{\alpha(\alpha-1)}{2!}<1$.

This implies that

$$\|R\|_2=\rho(R)\le\frac{K\tau h^{-\alpha}}{2\left|\cos\frac{\alpha\pi}{2}\right|}, \tag{4.26}$$

since R is a real and symmetric matrix.

Now, the eigenvalues of the tridiagonal matrix T are given by [51]

$$\lambda_v=1-\frac{K\tau h^{-\alpha}}{\cos\frac{\alpha\pi}{2}}\tilde{g}_1-\frac{K\tau h^{-\alpha}}{\cos\frac{\alpha\pi}{2}}(\tilde{g}_0+\tilde{g}_2)\cos\frac{v\pi}{m},\quad v=1,2,\ldots,m-1. \tag{4.27}$$

Now, let assume that $\overline{W}_l^k$ be the computed value of W_l^k of the explicit finite difference numerical scheme in Eq. (4.8), let $\varepsilon_l^k=\bar{W}_l^k-W_l^k$ and $\boldsymbol{Y}^k=[\varepsilon_1^k,\varepsilon_2^k,\ldots,\varepsilon_{m-1}^k]^T$.

Then, the vector $\boldsymbol{Y}^k$ satisfies the following equation

$$\boldsymbol{Y}^{k+1}=A\boldsymbol{Y}^k. \tag{4.28}$$

Thus, the explicit finite difference numerical scheme in Eq. (4.8) is stable if

$$\|A\|_2=\rho(A)\le\|T\|_2+\|R\|_2\le 1$$

This implies that

$$\left|1-\frac{K\tau h^{-\alpha}}{\cos\frac{\alpha\pi}{2}}\tilde{g}_1-\frac{K\tau h^{-\alpha}}{\cos\frac{\alpha\pi}{2}}(\tilde{g}_0+\tilde{g}_2)\cos\frac{(m-1)\pi}{m}\right|+\left|\frac{rK}{2\cos\frac{\alpha\pi}{2}}\right|\le 1, \tag{4.29}$$

After simplifications, from Eq. (4.29), we obtain

$$r \leq \frac{2\left|\cos\frac{\alpha\pi}{2}\right|}{K\left(\frac{\tilde{g}_1-(\tilde{g}_0+\tilde{g}_2)}{\operatorname{sgn}\left(\cos\frac{\alpha\pi}{2}\right)}+\tilde{g}_0\right)}, \tag{4.30}$$

as $h \to 0$, $m \to \infty$.

This completes the proof. ■

Theorem 4.2 *The numerical discretization scheme for the problem in* Eq. (4.21) *is unconditionally stable.*

Proof The matrix $\boldsymbol{A}_i$ in Eq. (4.18) can be written as

$$\boldsymbol{A}_i = \omega_i^{1-\alpha}\left(P + \frac{\nu\tau^\alpha}{2h}J\right), \quad i = 0, 1, 2, \ldots, k+1, \tag{4.31}$$

where

$$P = \begin{pmatrix} \frac{K_\alpha^\mu\tau^\alpha}{2}h^{-\mu}g_0 & \frac{K_\alpha^\mu\tau^\alpha}{2}h^{-\mu}g_{-1} & \ldots & \frac{K_\alpha^\mu\tau^\alpha}{2}h^{-\mu}g_{2-m} \\ \frac{K_\alpha^\mu\tau^\alpha}{2}h^{-\mu}g_1 & \frac{K_\alpha^\mu\tau^\alpha}{2}h^{-\mu}g_0 & \ldots & \frac{K_\alpha^\mu\tau^\alpha}{2}h^{-\mu}g_{3-m} \\ \ldots & \ldots & \ldots & \ldots \\ \frac{K_\alpha^\mu\tau^\alpha}{2}h^{-\mu}g_{m-2} & \frac{K_\alpha^\mu\tau^\alpha}{2}h^{-\mu}g_{m-3} & \ldots & \frac{K_\alpha^\mu\tau^\alpha}{2}h^{-\mu}g_0 \end{pmatrix},$$

$$J = \begin{pmatrix} -1 & 1 & 0 & \ldots & 0 \\ 0 & -1 & 1 & \ldots & 0 \\ \ldots & \ldots & \ldots & \ldots & \ldots \\ 0 & 0 & 0 & \ldots & -1 \end{pmatrix}.$$

Since $g_{-j} = g_j$, P is a $(m-1) \times (m-1)$ symmetric matrix and J is a $(m-1)\times(m-1)$ Jordan block matrix with eigenvalue -1.

Now, let λ_j be the eigenvalue of the matrix P. Then, according to the Gerschgorin circle theorem [50], we have

$$\left|\lambda_j - \frac{K_\alpha^\mu\tau^\alpha}{2}h^{-\mu}g_0\right| \leq \frac{K_\alpha^\mu\tau^\alpha}{2}h^{-\mu}\sum_{\substack{k=1 \\ k\neq i}}^{m-1}|g_{i-k}| < \frac{K_\alpha^\mu\tau^\alpha}{2}h^{-\mu}g_0, \tag{4.32}$$

where $\sum_{\substack{k=-\infty \\ k\neq 0}}^{\infty}|g_k| = g_0$.

This implies that

$$0 < \lambda_j < K_\alpha^\mu \tau^\alpha h^{-\mu} g_0. \tag{4.33}$$

Thus, the eigenvalue of $\boldsymbol{A}_i$ satisfies the following range

$$-\omega_i^{1-\alpha} \frac{\nu\tau^\alpha}{h} < \lambda(\boldsymbol{A}_i) < \omega_i^{1-\alpha} K_\alpha^\mu \tau^\alpha h^{-\mu} g_0$$

Therefore, we obtain

$$\rho(\boldsymbol{A}_i) < \omega_i^{1-\alpha} K_\alpha^\mu \tau^\alpha h^{-\mu} g_0 + \omega_i^{1-\alpha} \frac{\nu\tau^\alpha}{2h}. \tag{4.34}$$

Now, let assume that $\bar{W}_l^k$ be the computed value of W_l^k of the second-order accurate implicit numerical scheme in Eq. (4.16), let $\varepsilon_l^k = \bar{W}_l^k - W_l^k$ and $\boldsymbol{Y}^k = [\varepsilon_1^k, \varepsilon_2^k, \ldots, \varepsilon_{m-1}^k]^T$.

Then, the vector $\boldsymbol{Y}^k$ satisfies the following equation

$$\begin{aligned} \boldsymbol{Y}^{k+1} = {} & (\boldsymbol{I}+\boldsymbol{A}_0)^{-1}(\boldsymbol{I}-\boldsymbol{A}_0-\boldsymbol{A}_1)\boldsymbol{Y}^k - (\boldsymbol{I}+\boldsymbol{A}_0)^{-1}(\boldsymbol{A}_1+\boldsymbol{A}_2)\boldsymbol{Y}^{k-1} \\ & - (\boldsymbol{I}+\boldsymbol{A}_0)^{-1}(\boldsymbol{A}_2+\boldsymbol{A}_3)\boldsymbol{Y}^{k-2} - \cdots - (\boldsymbol{I}+\boldsymbol{A}_0)^{-1}(\boldsymbol{A}_k+\boldsymbol{A}_{k+1})\boldsymbol{Y}^0. \end{aligned} \tag{4.35}$$

Therefore, we obtain

$$\begin{aligned} \left\|\boldsymbol{Y}^{k+1}\right\|_2 \le {} & \left\|(\boldsymbol{I}+\boldsymbol{A}_0)^{-1}(\boldsymbol{I}-\boldsymbol{A}_0-\boldsymbol{A}_1)\right\|_2 \left\|\boldsymbol{Y}^k\right\|_2 + \left\|(\boldsymbol{I}+\boldsymbol{A}_0)^{-1}(\boldsymbol{A}_1+\boldsymbol{A}_2)\right\|_2 \left\|\boldsymbol{Y}^{k-1}\right\|_2 \\ & + \left\|(\boldsymbol{I}+\boldsymbol{A}_0)^{-1}(\boldsymbol{A}_2+\boldsymbol{A}_3)\right\|_2 \left\|\boldsymbol{Y}^{k-2}\right\|_2 + \cdots + \left\|(\boldsymbol{I}+\boldsymbol{A}_0)^{-1}(\boldsymbol{A}_k+\boldsymbol{A}_{k+1})\right\|_2 \left\|\boldsymbol{Y}^0\right\|_2. \end{aligned} \tag{4.36}$$

Now, without loss of generality, there exists $\alpha_i \in \mathsf{R}^+$, $i = 0, 1, \ldots, k$ such that

$$\begin{aligned} & \left\|(\boldsymbol{I}+\boldsymbol{A}_0)^{-1}(\boldsymbol{I}-\boldsymbol{A}_0-\boldsymbol{A}_1)\right\|_2 = [\rho([(\boldsymbol{I}+\boldsymbol{A}_0)^{-1}(\boldsymbol{I}-\boldsymbol{A}_0-\boldsymbol{A}_1)]^T[(\boldsymbol{I}+\boldsymbol{A}_0)^{-1}(\boldsymbol{I}-\boldsymbol{A}_0-\boldsymbol{A}_1)])]^{1/2} \le \alpha_k, \\ & \left\|(\boldsymbol{I}+\boldsymbol{A}_0)^{-1}(\boldsymbol{A}_1+\boldsymbol{A}_2)\right\|_2 = [\rho([(\boldsymbol{I}+\boldsymbol{A}_0)^{-1}(\boldsymbol{A}_1+\boldsymbol{A}_2)]^T[(\boldsymbol{I}+\boldsymbol{A}_0)^{-1}(\boldsymbol{A}_1+\boldsymbol{A}_2)])]^{1/2} \le \alpha_{k-1}, \\ & \ldots, \\ & \left\|(\boldsymbol{I}+\boldsymbol{A}_0)^{-1}(\boldsymbol{A}_k+\boldsymbol{A}_{k+1})\right\|_2 = [\rho([(\boldsymbol{I}+\boldsymbol{A}_0)^{-1}(\boldsymbol{A}_k+\boldsymbol{A}_{k+1})]^T[(\boldsymbol{I}+\boldsymbol{A}_0)^{-1}(\boldsymbol{A}_k+\boldsymbol{A}_{k+1})])]^{1/2} \le \alpha_0. \end{aligned} \tag{4.37}$$

Consequently, we obtain

$$\left\|\boldsymbol{Y}^{k+1}\right\|_2 \le \alpha_k \left\|\boldsymbol{Y}^k\right\|_2 + \alpha_{k-1} \left\|\boldsymbol{Y}^{k-1}\right\|_2 + \alpha_{k-2} \left\|\boldsymbol{Y}^{k-2}\right\|_2 + \cdots + \alpha_0 \left\|\boldsymbol{Y}^0\right\|_2. \tag{4.38}$$

Hence, we conclude that

$$\left\|\boldsymbol{Y}^{k+1}\right\|_2 \leq \alpha_0(\alpha_1+1)(\alpha_2+1)\ldots(\alpha_k+1)\left\|\boldsymbol{Y}^0\right\|_2. \tag{4.39}$$

Thus, the second-order accurate implicit numerical scheme in Eq. (4.16) for the problem (4.21) is unconditionally stable. ■

Theorem 4.3 *Assuming that the problem in* Eq. (4.21) *has a smooth exact solution* $W_l^n = W(x_l, t_n) \in \Lambda(\Omega)$ *and* $\bar{W}_l^n$ *be the numerically computed solution of the second-order implicit numerical scheme in* Eq. (4.15). *Then, the numerical solution* $\bar{W}_l^n$ *unconditionally converges to* W_l^n *as* h *and* τ *tend to zero.*

Proof Let the error at the grid point (x_l, t_k) defined by $e_l^k = \bar{W}_l^k - W_l^k$ and $\boldsymbol{E}^k = (e_1^k, e_2^k, \ldots, e_{m-1}^k)^T$. Then, from Eqs. (4.15) and (4.16) for problem 4.2, we have

$$\begin{aligned}\frac{\mathrm{e}_l^{k+1}-\mathrm{e}_l^k}{\tau} &= -\frac{v}{2}\tau^{\alpha-1}\sum_{r=0}^{k}\omega_r^{1-\alpha}\left(\frac{\mathrm{e}_{l+1}^{k-r}-\mathrm{e}_l^{k-r}}{h}\right) - \frac{v}{2}\tau^{\alpha-1}\sum_{r=1}^{k+1}\omega_r^{1-\alpha}\left(\frac{\mathrm{e}_{l+1}^{k+1-r}-\mathrm{e}_l^{k+1-r}}{h}\right)\\ &\quad -\frac{K_\alpha^\mu\tau^{\alpha-1}}{2}h^{-\mu}\sum_{r=0}^{k}\omega_r^{1-\alpha}\sum_{i=l-m}^{l}g_i\mathrm{e}_{l-i}^{k-r}\\ &\quad -\frac{K_\alpha^\mu\tau^{\alpha-1}}{2}h^{-\mu}\sum_{r=0}^{k+1}\omega_r^{1-\alpha}\sum_{i=l-m}^{l}g_i\mathrm{e}_{l-i}^{k+1-r}+O(\tau^2+h^2).\end{aligned} \tag{4.40}$$

Now, Eq. (4.40) can be written in the following matrix form

$$\begin{aligned}(\boldsymbol{I}+\boldsymbol{A}_0)\boldsymbol{E}^{k+1} &= (\boldsymbol{I}-\boldsymbol{A}_0-\boldsymbol{A}_1)\boldsymbol{E}^k-(\boldsymbol{A}_1+\boldsymbol{A}_2)\boldsymbol{E}^{k-1}\\ &\quad -(\boldsymbol{A}_2+\boldsymbol{A}_3)\boldsymbol{E}^{k-2}-\cdots-(\boldsymbol{A}_k+\boldsymbol{A}_{k+1})\boldsymbol{E}^0+\boldsymbol{C}_1\tau(\tau^2+h^2)\boldsymbol{I}.\end{aligned} \tag{4.41}$$

Thus, we have

$$\begin{aligned}\boldsymbol{E}^{k+1} &= (\boldsymbol{I}+\boldsymbol{A}_0)^{-1}(\boldsymbol{I}-\boldsymbol{A}_0-\boldsymbol{A}_1)\boldsymbol{E}^k-(\boldsymbol{I}+\boldsymbol{A}_0)^{-1}(\boldsymbol{A}_1+\boldsymbol{A}_2)\boldsymbol{E}^{k-1}\\ &\quad -(\boldsymbol{I}+\boldsymbol{A}_0)^{-1}(\boldsymbol{A}_2+\boldsymbol{A}_3)\boldsymbol{E}^{k-2}-\cdots-(\boldsymbol{I}+\boldsymbol{A}_0)^{-1}(\boldsymbol{A}_k+\boldsymbol{A}_{k+1})\boldsymbol{E}^0\\ &\quad +\boldsymbol{C}_1\tau(\tau^2+h^2)(\boldsymbol{I}+\boldsymbol{A}_0)^{-1}.\end{aligned} \tag{4.42}$$

Hence, we obtain

$$\begin{aligned}\left\|\boldsymbol{E}^{k+1}\right\|_2 &\leq \left\|(\boldsymbol{I}+\boldsymbol{A}_0)^{-1}(\boldsymbol{I}-\boldsymbol{A}_0-\boldsymbol{A}_1)\right\|_2\left\|\boldsymbol{E}^k\right\|_2+\left\|(\boldsymbol{I}+\boldsymbol{A}_0)^{-1}(\boldsymbol{A}_1+\boldsymbol{A}_2)\right\|_2\left\|\boldsymbol{E}^{k-1}\right\|_2\\ &\quad +\left\|(\boldsymbol{I}+\boldsymbol{A}_0)^{-1}(\boldsymbol{A}_2+\boldsymbol{A}_3)\right\|_2\left\|\boldsymbol{E}^{k-2}\right\|_2+\cdots+\left\|(\boldsymbol{I}+\boldsymbol{A}_0)^{-1}(\boldsymbol{A}_k+\boldsymbol{A}_{k+1})\right\|_2\left\|\boldsymbol{E}^0\right\|_2\\ &\quad +C_1\tau(\tau^2+h^2)\left\|(\boldsymbol{I}+\boldsymbol{A}_0)^{-1}\right\|_2 \leq \alpha_0(\alpha_1+1)(\alpha_2+1)\ldots(\alpha_k+1)\left\|\boldsymbol{E}^0\right\|_2\\ &\quad +C_1\tau(\tau^2+h^2)\left\|(\boldsymbol{I}+\boldsymbol{A}_0)^{-1}\right\|_2 < \alpha_0(\alpha_1+1)(\alpha_2+1)\ldots(\alpha_k+1)\left\|\boldsymbol{E}^0\right\|_2\\ &\quad +\frac{C_1\tau(\tau^2+h^2)}{\left(1-\frac{v\tau^2}{h}\omega_0\right)} \leq CT(\tau^2+h^2).\end{aligned}$$

Consequently, $\left\|\boldsymbol{E}^{k+1}\right\|_2 \to 0$ as $\tau \to 0$, $h \to 0$. This completes the proof. ■

4.4 Soliton Solutions of a Nonlinear and Nonlocal Sine-Gordon Equation Involving Riesz Space Fractional Derivative

In the present section, a new semi-numerical technique MHAM-FT method has been proposed to obtain the approximate solution of nonlocal fractional sine-Gordon equation (SGE). The fractional SGE with nonlocal Riesz derivative operator has been first time solved by MHAM-FT method.

4.4.1 Basic Idea of Modified Homotopy Analysis Method with Fourier Transform

Let us focus a brief overview of modified homotopy analysis method with Fourier transform (MHAM-FT). Consider the following fractional differential equation

$$N[u(x,t)] = 0, \tag{4.43}$$

where N is a nonlinear differential operator containing Riesz fractional derivative defined in Eq. (1.18) of Chap. 1, x and t denote independent variables, and $u(x,t)$ is an unknown function.

Then, applying Fourier transform Eq. (4.43) has been reduced to the following Fourier transformed differential equation

$$N[\hat{u}(k,t)] = 0, \tag{4.44}$$

where $\hat{u}(k,t)$ is the Fourier transform of $u(x,t)$.

According to HAM, the zeroth-order deformation equation of Eq. (4.44) reads as

$$(1-p)L[\phi(k,t;p) - \hat{u}_0(k,t)] = p\hbar N[\phi(k,t;p)], \tag{4.45}$$

where L is an auxiliary linear operator, $\phi(k,t;p)$ is an unknown function, $\hat{u}_0(k,t)$ is an initial guess of $\hat{u}(k,t)$, $\hbar \neq 0$ is an auxiliary parameter, and $p \in [0,1]$ is the embedding parameter. In this proposed MHAM-FT, the nonlinear term appeared in expression for nonlinear operator form has been expanded using Adomian's type of polynomials as $\sum_{n=0}^{\infty} A_n p^n$ [52].

Obviously, when $p = 0$ and $p = 1$, we have

$$\phi(k,t;0) = \hat{u}_0(k,t), \phi(k,t;1) = \hat{u}(k,t), \tag{4.46}$$

respectively. Thus, as p increases from 0 to 1, the solution $\phi(k,t;p)$ varies from the initial guess $\hat{u}_0(k,t)$ to the solution $\hat{u}(k,t)$. Expanding $\phi(x,t;p)$ in Taylor series with respect to the embedding parameter p, we have

$$\phi(k,t;p) = \hat{u}_0(k,t) + \sum_{m=1}^{+\infty} p^m \hat{u}_m(k,t), \tag{4.47}$$

where $\hat{u}_m(k,t) = \frac{1}{m!}\frac{\partial^m}{\partial p^m}\phi(k,t;p)\Big|_{p=0}$.

The convergence of the series (4.47) depends upon the auxiliary parameter $\hbar$. If it is convergent at $p = 1$, we have

$$\hat{u}(k,t) = \hat{u}_0(k,t) + \sum_{m=1}^{+\infty} \hat{u}_m(k,t),$$

which must be one of the solutions of the original nonlinear equation.

Differentiating the zeroth-order deformation Eq. (4.45) m times with respect to p and then setting $p = 0$ and finally dividing them by $m!$, we obtain the following mth-order deformation equation

$$L[\hat{u}_m(k,t) - \chi_m \hat{u}_{m-1}(k,t)] = \hbar \Re_m(\hat{u}_0, \hat{u}_1, \ldots, \hat{u}_{m-1}), \tag{4.48}$$

where

$$\Re_m(\hat{u}_0, \hat{u}_1, \ldots, \hat{u}_{m-1}) = \frac{1}{(m-1)!}\frac{\partial^{m-1} N[\phi(k,t;p)]}{\partial p^{m-1}}\Big|_{p=0}$$

and

$$\chi_m = \begin{cases} 1, & m > 1 \\ 0, & m \leq 1 \end{cases}. \tag{4.49}$$

It should be noted that $\hat{u}_m(k,t)$ for $m \geq 1$ is governed by the linear Eq. (4.48) which can be solved by symbolic computational software. Then, by applying inverse Fourier transformation, we can get each component $u_m(x,t)$ of the approximate series solution

$$u(x,t) = \sum_{m=0}^{\infty} u_m(x,t).$$

In the present analysis, for reducing Riesz space fractional differential equation to ordinary differential equation, we applied here Fourier transform. In this modified homotopy analysis method, with Fourier transform (MHAM-FT), we applied the inverse Fourier transform for getting the solution of Riesz space fractional differential equation. This MHAM-FT technique has been first time proposed by the author.

4.4.2 Implementation of the MHAM-FT Method for Approximate Solution of Nonlocal Fractional SGE

In this section, we first consider two examples for the application of MHAM-FT for the solution of nonlocal fractional SGE Eq. (4.1).

Example 4.3 In this example, we shall find the approximate solution of the nonlocal fractional SGE Eq. (4.1) with given initial conditions [52–54]

$$u(x,0) = 0, u_t(x,0) = 4 \text{ sec } hx \tag{4.50}$$

Then, using Eq. (1.18) of Chap. 1 and applying Fourier transform on Eqs. (4.1) and (4.50), we get

$$\hat{u}_{tt}(k,t) + |k|^{\alpha}\hat{u}(k,t) + \mathsf{F}(\sin u) = 0, \tag{4.51}$$

with initial conditions

$$\hat{u}(k,0) = 0, \quad \hat{u}_t(k,0) = 2\sqrt{2\pi}\sec h\left(\frac{k\pi}{2}\right), \tag{4.52}$$

where F denotes the Fourier transform and k is called the transform parameter for Fourier transform.

Expanding $\phi(k,t;p)$ in Taylor series with respect to p, we have

$$\phi(k,t;p) = \hat{u}_0(k,t) + \sum_{m=1}^{+\infty} p^m \hat{u}_m(k,t), \tag{4.53}$$

where

$$\hat{u}_m(k,t) = \frac{1}{m!}\frac{\partial^m \phi(k,t;p)}{\partial p^m}\bigg|_{p=0}.$$

To obtain the approximate solution of the fractional SGE in Eq. (4.51), we choose the linear operator

$$L[\phi(k,t;p)] = \phi_{tt}(k,t;p). \tag{4.54}$$

From Eq. (4.44), we define a nonlinear operator as

$$N[\phi(k,t;p)] = \phi_{tt}(k,t;p) + |k|^{\alpha}\phi(k,t;p) + \mathsf{F}(\sin(\phi(k,t;p))), \tag{4.55}$$

where the nonlinear term $\sin(\phi(k,t;p))$ is expanded in terms of Adomian-like polynomials.

The nonlinear term $\sin(\phi(k,t;p))$ has been taken as

$$\sin(\phi(k,t;p)) = \sum_{n=0}^{\infty} p^n A_n,$$

where $A_n = \frac{1}{n!}\frac{\partial^n}{\partial p^n}\left(\sin\left(\hat{u}_0(k,t) + \sum_{m=1}^{+\infty} p^m \hat{u}_m(k,t)\right)\right)_{p=0}, n \geq 0.$

Using Eq. (4.45), we construct the so-called zeroth-order deformation equation

$$(1-p)L[\phi(k,t;p) - \hat{u}_0(k,t)] = p\hbar N[\phi(k,t;p)]. \tag{4.56}$$

Obviously, when $p = 0$ and $p = 1$, Eq. (4.56) yields

$$\phi(k,t;0) = \hat{u}_0(k,t); \phi(k,t;1) = \hat{u}(k,t).$$

Therefore, as the embedding parameter p increases from 0 to 1, $\phi(k,t;p)$ varies from the initial guess to the exact solution $\hat{u}(k,t)$.

If the auxiliary linear operator, the initial guess, and the auxiliary parameter $\hbar$ are so properly chosen, the above series in Eq. (4.53) converges at $p = 1$, and we obtain

$$\hat{u}(k,t) = \phi(k,t;1) = \hat{u}_0(k,t) + \sum_{m=1}^{+\infty} \hat{u}_m(k,t). \tag{4.57}$$

According to Eq. (4.48), we have the mth-order deformation equation

$$L[\hat{u}_m(k,t) - \chi_m \hat{u}_{m-1}(k,t)] = \hbar \Re_m(\hat{u}_0, \hat{u}_1, \ldots, \hat{u}_{m-1}), m \geq 1, \tag{4.58}$$

where

$$\begin{aligned} \Re_m(\hat{u}_0, \hat{u}_1, \ldots, \hat{u}_{m-1}) &= \frac{1}{(m-1)!}\frac{\partial^{m-1}}{\partial p^{m-1}} N[\phi(k,t;p)]\Big|_{p=0} \\ &= \frac{\partial^2 \hat{u}_{m-1}(k,t;p)}{\partial t^2} + |k|^{\alpha}\hat{u}_{m-1}(k,t;p) + \mathsf{F}(A_{m-1}). \end{aligned} \tag{4.59}$$

Now, the solution of the mth-order deformation Eq. (4.58) for $m \geq 1$ becomes

$$\hat{u}_m(k,t) = \chi_m \hat{u}_{m-1}(k,t) + \hbar L^{-1}[\Re_m(\hat{u}_0, \hat{u}_1, \ldots, \hat{u}_{m-1})]. \tag{4.60}$$

From Eq. (4.60), we have the following equations

$$\begin{aligned}
\hat{u}_0(k,t) &= \hat{u}(k,0) + t\hat{u}_t(k,0),\\
\hat{u}_1(k,t) &= \hbar L^{-1}\left(\frac{\partial^2 \hat{u}_0(k,t;p)}{\partial t^2} + |k|^{\alpha}\hat{u}_0(k,t;p) + \mathsf{F}(A_0)\right),\\
\hat{u}_2(k,t) &= \hat{u}_1(k,t) + \hbar L^{-1}\left(\frac{\partial^2 \hat{u}_1(k,t;p)}{\partial t^2} + |k|^{\alpha}\hat{u}_1(k,t;p) + \mathsf{F}(A_1)\right),\\
\hat{u}_3(k,t) &= \hat{u}_2(k,t) + \hbar L^{-1}\left(\frac{\partial^2 \hat{u}_2(k,t;p)}{\partial t^2} + |k|^{\alpha}\hat{u}_2(k,t;p) + \mathsf{F}(A_2)\right),
\end{aligned} \tag{4.61}$$

and so on.

But here for the sake of efficient computation for the nonlinear term, the above scheme in Eq. (4.61) has been modified in the following way

$$\begin{aligned}
\hat{u}_0(k,t) &= \hat{u}(k,0),\\
\hat{u}_1(k,t) &= t\hat{u}_t(k,0) + \hbar L^{-1}\left(\frac{\partial^2 \hat{u}_0(k,t;p)}{\partial t^2} + |k|^{\alpha}\hat{u}_0(k,t;p) + \mathsf{F}(A_0)\right),\\
\hat{u}_2(k,t) &= \hbar L^{-1}\left(\frac{\partial^2 \hat{u}_1(k,t;p)}{\partial t^2} + |k|^{\alpha}\hat{u}_1(k,t;p) + \mathsf{F}(A_1)\right),\\
\hat{u}_3(k,t) &= \hat{u}_2(k,t) + \hbar L^{-1}\left(\frac{\partial^2 \hat{u}_2(k,t;p)}{\partial t^2} + |k|^{\alpha}\hat{u}_2(k,t;p) + \mathsf{F}(A_2)\right),\\
\hat{u}_4(k,t) &= \hat{u}_3(k,t) + \hbar L^{-1}\left(\frac{\partial^2 \hat{u}_3(k,t;p)}{\partial t^2} + |k|^{\alpha}\hat{u}_3(k,t;p) + \mathsf{F}(A_3)\right),
\end{aligned} \tag{4.62}$$

and so on.

By putting the initial conditions in Eq. (4.52) into Eq. (4.62) and solving them, we now successively obtain

$$\hat{u}_0(k,t) = 0, \tag{4.63}$$

$$\hat{u}_1(k,t) = 2\sqrt{2\pi}t \sec h\left(\frac{k\pi}{2}\right), \tag{4.64}$$

$$\hat{u}_2(k,t) = \hbar\left(\frac{1}{3}\sqrt{2\pi}t^3 \sec h\left(\frac{k\pi}{2}\right) + \frac{1}{3}\sqrt{2\pi}t^3|k|^{\alpha}\sec h\left(\frac{k\pi}{2}\right)\right), \tag{4.65}$$

and so on.

Then, by applying the inverse Fourier transform of Eqs. (4.63)–(4.65), we determine

$$
\begin{aligned}
u_0(x,t) &= 0,\\
u_1(x,t) &= 4t\ \text{sec}\ hx,\\
u_2(x,t) &= \frac{1}{3}t^3\hbar\Big(2\ \text{sec}\ hx + 2^{-\alpha}\pi^{-1-\alpha}\Gamma(1+\alpha)\Big(\zeta\Big(1+\alpha,\frac{\pi-2ix}{4\pi}\Big)+\zeta\Big(1+\alpha,\frac{\pi+2ix}{4\pi}\Big)\\
&\quad -\zeta\Big(1+\alpha,\frac{3}{4}-\frac{ix}{2\pi}\Big)-\zeta\Big(1+\alpha,\frac{3}{4}+\frac{ix}{2\pi}\Big)\Big)\Big),
\end{aligned}
$$

and so on, where $\zeta(s,a)=\sum_{k=0}^{\infty}\frac{1}{(k+a)^s}$ is called Hurwitz zeta function which is a generalization of the Riemann zeta function $\zeta(s)$ and also known as the generalized zeta function.

In this manner, the other components of the homotopy series can be easily obtained by which $u(x,t)$ can be evaluated in a series form as

$$
\begin{aligned}
u(x,t) &= u_0(x,t)+u_1(x,t)+u_2(x,t)+\cdots\\
&= 4t\ \text{sec}\ hx+\frac{1}{3}t^3\hbar\Big(2\ \text{sec}\ hx+2^{-\alpha}\pi^{-1-\alpha}\Gamma(1+\alpha)\Big(\zeta\Big(1+\alpha,\frac{\pi-2ix}{4\pi}\Big)\\
&\quad +\zeta\Big(1+\alpha,\frac{\pi+2ix}{4\pi}\Big)-\zeta\Big(1+\alpha,\frac{3}{4}-\frac{ix}{2\pi}\Big)\\
&\quad -\zeta\Big(1+\alpha,\frac{3}{4}+\frac{ix}{2\pi}\Big)\Big)\Big)+\cdots.
\end{aligned}
\tag{4.66}
$$

Example 4.4 In this case, we shall find the approximate solution of the nonlocal fractional SGE Eq. (4.1) with given initial conditions [55–57]

$$
u(x,0)=\pi+\varepsilon\cos(\mu x),\quad u_t(x,0)=0. \tag{4.67}
$$

Then, using Eq. (1.18) of Chap. 1 and applying Fourier transform on Eqs. (4.1) and (4.67), we get

$$
\hat{u}_{tt}(k,t)+|k|^{\alpha}\hat{u}(k,t)+\mathsf{F}(\sin u)=0, \tag{4.68}
$$

with initial conditions

$$
\hat{u}(k,0)=\sqrt{2}\pi^{3/2}\delta(k)+\sqrt{\frac{\pi}{2}}\varepsilon\delta(k-\mu)+\sqrt{\frac{\pi}{2}}\varepsilon\delta(k+\mu),\quad \hat{u}_t(k,0)=0, \tag{4.69}
$$

where F denotes the Fourier transform, k is called the transform parameter for Fourier transform, and $\delta(.)$ denotes the Dirac delta function.

Analogous to arguments as discussed in Example 4.3, we may obtain the following equations

$$\begin{aligned}
\hat{u}_0(k,t) &= \sqrt{2}\pi^{3/2}\delta(k),\\
\hat{u}_1(k,t) &= \sqrt{\frac{\pi}{2}}\varepsilon\delta(k-\mu)+\sqrt{\frac{\pi}{2}}\varepsilon\delta(k+\mu)+\hbar L^{-1}\left(\frac{\partial^2\hat{u}_0(k,t;p)}{\partial t^2}+|k|^{\alpha}\hat{u}_0(k,t;p)+\mathsf{F}(A_0)\right),\\
\hat{u}_2(k,t) &= \hbar L^{-1}\left(\frac{\partial^2\hat{u}_1(k,t;p)}{\partial t^2}+|k|^{\alpha}\hat{u}_1(k,t;p)+\mathsf{F}(A_1)\right),\\
\hat{u}_3(k,t) &= \hat{u}_2(k,t)+\hbar L^{-1}\left(\frac{\partial^2\hat{u}_2(k,t;p)}{\partial t^2}+|k|^{\alpha}\hat{u}_2(k,t;p)+\mathsf{F}(A_1)\right),\\
\hat{u}_4(k,t) &= \hat{u}_3(k,t)+\hbar L^{-1}\left(\frac{\partial^2\hat{u}_3(k,t;p)}{\partial t^2}+|k|^{\alpha}\hat{u}_3(k,t;p)+\mathsf{F}(A_3)\right),
\end{aligned} \tag{4.70}$$

and so on.

Solving Eq. (4.70), we now successively obtain

$$\hat{u}_0(k,t) = \sqrt{2}\pi^{3/2}\delta(k), \tag{4.71}$$

$$\hat{u}_1(k,t) = \sqrt{\frac{\pi}{2}}\varepsilon\delta(k-\mu)+\sqrt{\frac{\pi}{2}}\varepsilon\delta(k+\mu), \tag{4.72}$$

$$\begin{aligned}
\hat{u}_2(k,t) = \hbar\Bigg(&-\frac{1}{2}\sqrt{\frac{\pi}{2}}t^2\varepsilon\delta(k-\mu)+\frac{1}{2}\sqrt{\frac{\pi}{2}}t^2\varepsilon|k|^{\alpha}\delta(k-\mu)-\frac{1}{2}\sqrt{\frac{\pi}{2}}t^2\varepsilon\delta(k+\mu)\\
&+\frac{1}{2}\sqrt{\frac{\pi}{2}}t^2\varepsilon|k|^{\alpha}\delta(k+\mu)\Bigg),
\end{aligned} \tag{4.73}$$

and so on.

Then, by applying the inverse Fourier transform of Eqs. (4.71)–(4.73), we have

$$\begin{aligned}
u_0(x,t) &= \pi,\\
u_1(x,t) &= \varepsilon\cos(\mu x),\\
u_2(x,t) &= \frac{1}{2}t^2\varepsilon\hbar(-1+\mu^{\alpha})\cos(\mu x),\\
u_3(x,t) &= \frac{1}{24}t^2\varepsilon\hbar(-1+\mu^{\alpha})\left(12-\left(-12+t^2\right)\hbar+t^2\hbar\mu^{\alpha}\right)\cos(\mu x),
\end{aligned}$$

and so on.

In this manner, the other components of the homotopy series can be easily obtained by which $u(x,t)$ can be evaluated in a series form as

$$u(x,t) = u_0(x,t) + u_1(x,t) + u_2(x,t) + \cdots$$
$$= \frac{1}{24}\left(24\pi + \varepsilon\left(24 + 12t^2\hbar(2+\hbar)(-1+\mu^\alpha) + t^4\hbar^2(-1+\mu^\alpha)^2\right)\cos(\mu x)\right) + \cdots. \tag{4.74}$$

The After-Treatment Technique

Padé approximation may be used to enable us in order to increase the radius of convergence of the series. This method can be used for analytic continuation of a series for extending the radius of convergence. A Padé approximant is the ratio of two polynomials constructed from the coefficients of the Maclaurin series expansion of a function. Given a function $f(t)$ expanded in a Maclaurin series $f(t) = \sum_{n=0}^{\infty} c_n t^n$, we can use the coefficients of the series to represent the function by a ratio of two polynomials denoted by $[L/M]$ and called the Padé approximant, i.e.,

$$\left[\frac{L}{M}\right] = \frac{P_L(t)}{Q_M(t)}, \tag{4.75}$$

where $P_L(t)$ is a polynomial of degree at most L and $Q_M(t)$ is a polynomial of degree at most M. The polynomials $P_L(t)$ and $Q_M(t)$ have no common factors. Such rational fractions are known to have remarkable properties of analytic continuation. Even though the series has a finite region of convergence, we can obtain the limit of the function as $t \to \infty$ if $L = M$.

In case of Example 4.4, $u(x,t)$ can be evaluated in a series form as

$$u(x,t) = \frac{1}{24}\left(24\pi + \varepsilon\left(24 + 12t^2\hbar(2+\hbar)(-1+\mu^\alpha) + t^4\hbar^2(-1+\mu^\alpha)^2\right)\cos(\mu x)\right). \tag{4.76}$$

Putting $x = 0.05, \hbar = -1, \varepsilon = 0.01, \mu = \frac{1}{\sqrt{2}}$ and $\alpha = 2$ and applying Padé approximant [5/5] to Eq. (4.76), we obtain

$$u(0.05,t) = \left(\frac{3.15158 - 0.066294\,t^2 + 0.00072717\,t^4}{1 - 0.021828\,t^2 + 0.00021501\,t^4}\right). \tag{4.77}$$

The $\hbar$-Curve and Numerical Simulations for MHAM-FT Method and Discussions

As pointed out by Liao [58] in general, by means of the so-called $\hbar$-curve, it is straightforward to choose a proper value of $\hbar$ which ensures that the solution series is convergent.

To investigate the influence of $\hbar$ on the solution series, we plot the so-called $\hbar$-curve of partial derivatives of $u(x,t)$ at $(0,0)$ obtained from the sixth-order MHAM-FT solutions as shown in Fig. 4.7. In this way, it is found that our series converges when $\hbar = -1$.

In this present numerical experiment, Eq. (4.66) obtained by MHAM-FT has been used to draw the graphs as shown in Fig. 4.8 for $\alpha = 1.75$. The numerical solutions of Riesz fractional SGE in Eq. (4.1) have been shown in Fig. 4.8 with the help of third-order approximation for the homotopy series solution of $u(x,t)$, when $\hbar = -1$.

In this present analysis, Eq. (4.74) obtained by MHAM-FT has been used to draw the graphs as shown in Fig. 4.9 for fractional-order value $\alpha = 1.75$. The numerical solutions of fractional SGE Eq. (4.1) have been shown in Fig. 4.9 with the help of sixth-order approximation for the homotopy series solution of $u(x,t)$, when $\hbar = -1$.

In order to examine the numerical results obtained by the proposed method, both Examples 4.3 and 4.4 have been solved by a numerical method involving Chebyshev polynomial. The comparison of the approximate solutions for fractional SGE Eq. (4.1) given in Examples 4.3 and 4.4 has been exhibited in Tables 4.1 and 4.4 which are constructed using the results obtained by MHAM and Chebyshev polynomial at different values of x and t taking $\alpha = 1.75$ and 1.5, respectively. Similarly, Tables 4.2 and 4.5 show the comparison of absolute errors for classical SGE given in Examples 4.3 and 4.4, respectively. To show the accuracy of the proposed MHAM over Chebyshev polynomials, L_2 and L_∞ error norms for classical order SGE given in Examples 4.3 and 4.4 have been presented in Tables 4.3 and 4.6, respectively. Agreement between present numerical results obtained by MHAM with Chebyshev polynomials and exact solutions appear very satisfactory through illustrations in Tables 4.1, 4.2, 4.3, 4.4, and 4.6. The following Fig. 4.10

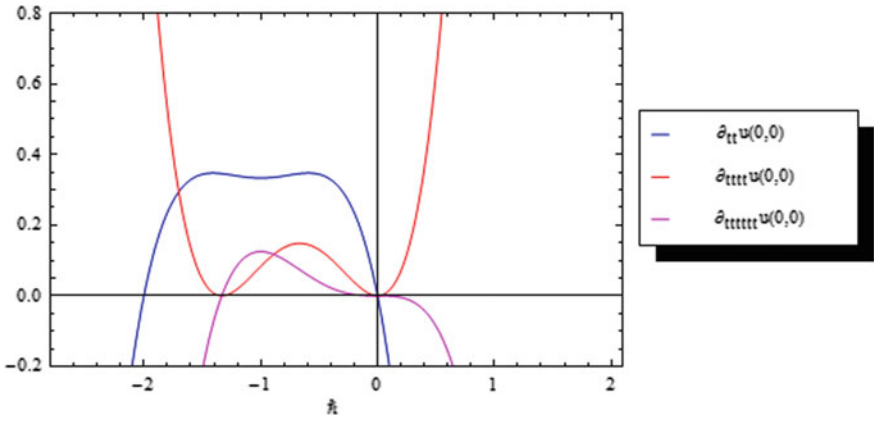

Fig. 4.7 $\hbar$-curve for partial derivatives of $u(x,t)$ at $(0,0)$ for the sixth-order MHAM-FT solution when $\alpha = 2$

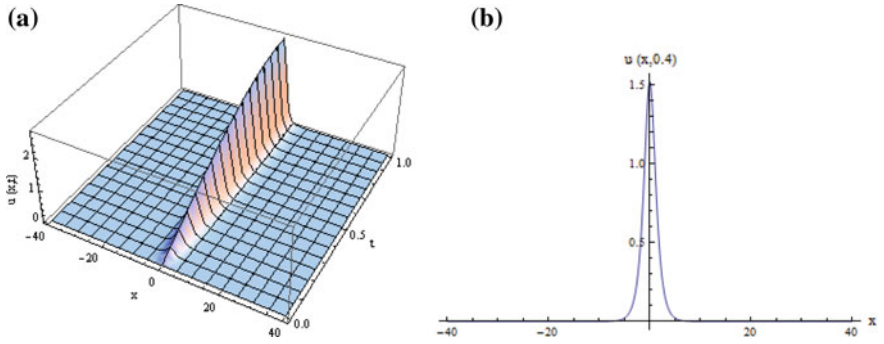

Fig. 4.8 **a** MHAM-FT method solution for $u(x,t)$ and **b** corresponding solution for $u(x,t)$ when $t = 0.4$

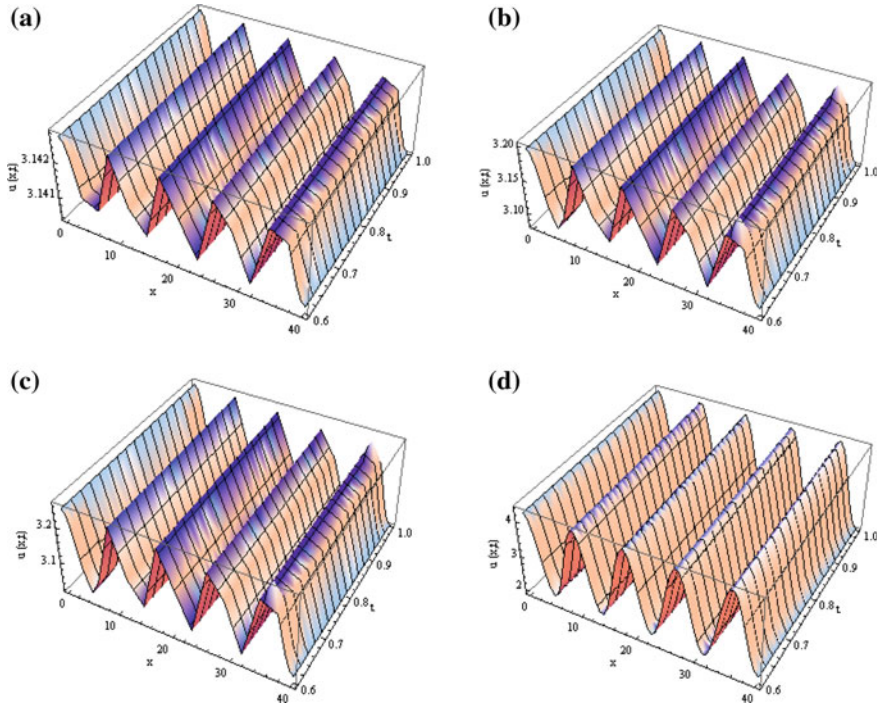

Fig. 4.9 Numerical results for $u(x,t)$ obtained by MHAM-FT for **a** $\varepsilon = 0.001$, **b** $\varepsilon = 0.05$, **c** $\varepsilon = 0.1$, and **d** $\varepsilon = 1.0$

demonstrates a graphical comparison of the numerical solutions for $u(0.05,t)$ obtained by MHAM-FT and Padé approximation with regard to the exact solution for Example 4.3.

Table 4.1 Comparison of approximate solutions obtained by modified homotopy analysis method and Chebyshev polynomial of second kind for fractional SGE Eq. (4.1) given in Example 4.3 at various points of x and t taking $\alpha = 1.75$ and 1.5 with $\hbar = -1$

x	$\alpha = 1.75$				$\alpha = 1.5$			
	$t = 0.01$		$t = 0.02$		$t = 0.01$		$t = 0.02$	
	$u_{\text{Chebyshev}}$	u_{MHAM}	$u_{\text{Chebyshev}}$	u_{MHAM}	$u_{\text{Chebyshev}}$	u_{MHAM}	$u_{\text{Chebyshev}}$	u_{MHAM}
0.01	0.033828	0.039996	0.0600056	0.079986	0.034480	0.039996	0.059515	0.079986
0.02	0.018271	0.039991	0.0571674	0.079974	0.033566	0.039991	0.062218	0.079974
0.03	0.010936	0.039981	0.0562336	0.079954	0.033364	0.039981	0.064389	0.079954
0.04	0.009624	0.039966	0.0566734	0.079926	0.033664	0.039966	0.066099	0.079926
0.05	0.012513	0.039948	0.0580476	0.079890	0.034294	0.039948	0.067413	0.079890
0.06	0.018109	0.039926	0.0599977	0.079846	0.035114	0.039926	0.068388	0.079846
0.07	0.025213	0.039901	0.0622362	0.079794	0.036014	0.039901	0.069075	0.079794
0.08	0.032879	0.039871	0.0645376	0.079734	0.036907	0.039871	0.069521	0.079735
0.09	0.040384	0.039837	0.0667305	0.079667	0.037728	0.039837	0.069766	0.079667
0.1	0.047194	0.039799	0.0686896	0.079592	0.038433	0.039799	0.069845	0.079592

Table 4.2 Comparison of absolute errors obtained by modified homotopy analysis method and Chebyshev polynomial of second kind for SGE equation given in Example 4.3 at various points of x and t taking $\alpha = 2$ and $\hbar = -1$

x	t	$\lvert u_{\text{Exact}} - u_{\text{Chebyshev}} \rvert$	$\lvert u_{\text{Exact}} - u_{\text{MHAM}} \rvert$
0.02	0.02	1.45347E−5	2.55671E−9
0.04	0.02	1.46767E−5	2.54906E−9
0.06	0.02	1.48475E−5	2.53636E−9
0.08	0.02	1.50368E−5	2.51869E−9
0.1	0.02	1.52361E−5	2.49619E−9
0.02	0.04	5.26987E−5	8.17448E−8
0.04	0.04	5.32093E−5	8.15001E−8
0.06	0.04	5.38216E−5	8.10941E−8
0.08	0.04	5.45030E−5	8.05296E−8
0.1	0.04	5.52250E−5	7.98104E−8
0.02	0.06	1.07843E−5	6.19865E−7
0.04	0.06	1.08860E−4	6.18011E−7
0.06	0.06	1.10091E−4	6.14935E−7
0.08	0.06	1.11471E−4	6.10656E−7
0.1	0.06	1.12943E−4	6.05206E−7
0.02	0.08	1.75050E−4	2.60691E−6
0.04	0.08	1.76623E−4	2.59912E−6
0.06	0.08	1.78561E−4	2.58619E−6
0.08	0.08	1.80758E−4	2.56821E−6
0.1	0.08	1.83120E−4	2.54531E−6
0.02	0.1	2.50768E−4	7.93538E−6
0.04	0.1	2.52867E−4	7.91169E−6

(continued)

Table 4.2 (continued)

x	t	$\lvert u_{\text{Exact}} - u_{\text{Chebyshev}} \rvert$	$\lvert u_{\text{Exact}} - u_{\text{MHAM}} \rvert$
0.06	0.1	2.55516E−4	7.87237E−6
0.08	0.1	2.58561E−4	7.81770E−6
0.1	0.1	2.61864E−4	7.74804E−6

Table 4.3 L_2 and L_∞ error norm for SGE Eq. (4.1) given in Example 4.3 at various points of x and t taking $\alpha = 2$

t	MHAM		Chebyshev polynomial	
	L_2	L_∞	L_2	L_∞
0.02	5.6606E−9	2.55671E−9	3.32469E−5	1.52361E−5
0.04	1.80985E−7	8.17448E−8	1.20522E−4	5.52250E−5
0.06	1.37240E−6	6.19865E−7	2.46541E−4	1.12943E−4
0.08	5.77184E−6	2.60691E−6	3.99911E−4	1.83120E−4
0.10	1.75695E−5	7.93538E−6	5.72312E−4	2.61864E−4

Table 4.4 Comparison of approximate solutions obtained by modified homotopy analysis method and Chebyshev polynomial of second kind for fractional SGE Eq. (4.1) given in Example 4.4 at various points of x and t taking $\alpha = 1.75$ and 1.5 with $\hbar = -1$

x	$\alpha = 1.75$				$\alpha = 1.5$			
	$t = 0.01$		$t = 0.02$		$t = 0.01$		$t = 0.02$	
	$u_{\text{Chebyshev}}$	u_{MHAM}	$u_{\text{Chebyshev}}$	u_{MHAM}	$u_{\text{Chebyshev}}$	u_{MHAM}	$u_{\text{Chebyshev}}$	u_{MHAM}
0.10	3.13459	3.151570	3.08713	3.1515800	3.15003	3.151567	3.14319	3.15156847
0.15	3.15900	3.151536	3.18638	3.1515373	3.16211	3.151540	3.19226	3.15153726
0.20	3.16542	3.15149	3.20162	3.1514930	3.16066	3.151492	3.18787	3.15149362
0.25	3.15980	3.15144	3.18315	3.1514377	3.15390	3.151438	3.16158	3.15143760
0.30	3.15161	3.15137	3.15421	3.1513693	3.14879	3.15136	3.14129	3.15136928
0.35	3.14675	3.15129	3.13604	3.1512888	3.14823	3.15128	3.13897	3.15128874
0.40	3.14623	3.15120	3.13282	3.1511961	3.15131	3.15119	3.15122	3.15119609
0.45	3.14781	3.15109	3.13733	3.1510915	3.15506	3.15108	3.16632	3.15109143
0.50	3.14867	3.15097	3.14015	3.1509749	3.15662	3.150970	3.17283	3.15097489

Table 4.5 Absolute errors obtained by modified homotopy analysis method and Chebyshev polynomial of second kind for classical SGE equation given in Example 4.4 at various points of x and t taking $\hbar = -1$

x	t	$\lvert u_{\text{Chebyshev}} - u_{\text{MHAM}} \rvert$
0.2	0.2	5.09463E−5
0.4	0.2	8.84127E−5
0.6	0.2	1.48843E−4
0.8	0.2	2.20924E−4

(continued)

Table 4.5 (continued)

x	t	$\lvert u_{\text{Chebyshev}} - u_{\text{MHAM}} \rvert$
1.0	0.2	2.85454E−4
0.2	0.4	2.00397E−5
0.4	0.4	1.11716E−4
0.6	0.4	3.30001E−4
0.8	0.4	5.79195E−4
1.0	0.4	8.02329E−4
0.2	0.6	4.93420E−4
0.4	0.6	2.19299E−4
0.6	0.6	2.24080E−4
0.8	0.6	7.26968E−4
1.0	0.6	1.19255E−4
0.2	0.8	1.56021E−3
0.4	0.8	1.09038E−3
0.6	0.8	3.68090E−4
0.8	0.8	4.64603E−4
1.0	0.8	1.30778E−3
0.2	1.0	3.30232E−3
0.4	1.0	2.56352E−3
0.6	1.0	1.50743E−3
0.8	1.0	2.41294E−4
1.0	1.0	1.22502E−3

Table 4.6 L_2 and L_∞ error norm obtained by MHAM and Chebyshev polynomial with regard to HAM for SGE Eq. (4.1) given in Example 4.4 at various points of x and t taking $\varepsilon = 1$ and $\alpha = 2$

t	MHAM		Chebyshev polynomial	
	L_2	L_∞	L_2	L_∞
0.02	3.61832E−6	1.62617E−6	3.16274E−6	1.98279E−6
0.04	1.44585E−5	6.49802E−6	2.02068E−5	9.70659E−6
0.06	3.24763E−5	1.45956E−5	4.76627E−5	2.21017E−5
0.08	5.75978E−5	2.58855E−5	8.09011E−5	3.87676E−5
0.10	8.97196E−5	5.92957E−5	1.30016E−4	5.85008E−5

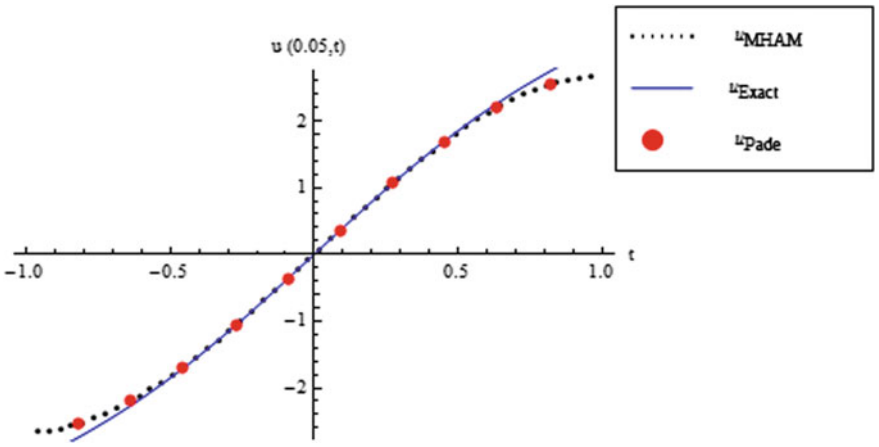

Fig. 4.10 Graphical comparison of the numerical solutions $u(0.05, t)$ obtained by MHAM-FT and Padé approximation with regard to the exact solution for Example 4.3

4.5 Conclusion

In the present chapter, shifted Grünwald approximation has been used in order to discretize the Riesz fractional diffusion equation. This equation has been solved by explicit finite difference method. The numerical solution of time and space Riesz fractional Fokker–Planck equation has been obtained from the discretization by fractional centered difference approximation of the Riesz space fractional derivative. The implicit finite difference method has been applied in order to solve the Riesz fractional Fokker–Planck equation. The above numerical schemes are quite accurate and efficient, and the numerical results demonstrated here exhibit the pretty good agreement with the exact solutions.

Moreover, in this chapter, a new semi-numerical technique MHAM-FT method has been proposed to obtain the approximate solution of nonlocal fractional SGE. The fractional SGE with nonlocal Riesz derivative operator has been first time solved by MHAM-FT method in order to justify the applicability of the proposed method. The approximate solutions obtained by MHAM-FT provide us with a convenient way to control the convergence of approximate series solution and solves the problem without any need for the discretization of the variables. To control the convergence of the solution, we can choose the proper values of $\hbar$; here we choose $\hbar = -1$. In order to examine the numerical results obtained by the proposed method, both Examples 4.3 and 4.4 have been solved by a numerical method involving Chebyshev polynomial. To show the accuracy of the proposed MHAM over Chebyshev polynomials, L_2 and L_∞ error norms for classical order SGE given in Examples 4.3 and 4.4 have been presented in Tables 4.3 and 4.6, respectively. Agreement between present numerical results obtained by MHAM with Chebyshev polynomials and exact solutions appears very satisfactory through

illustrations in Tables 4.1, 4.2, 4.3, 4.4, and 4.6. The proposed MHAM-FT method is very simple and efficient for solving the nonlinear fractional sine-Gordon equation with nonlocal Riesz derivative operator. Thus, the proposed MHAM-FT method can be elegantly applied for solving other Riesz fractional differential equations.

References

1. Wang, X., Liu, F., Chen, X.: Novel second-order accurate implicit numerical methods for the riesz space distributed-order advection-dispersion equations. Adv. Math. Phys. **2015**, 14 (2015). (Article ID 590435)
2. Saha Ray, S.: Exact solutions for time fractional diffusion method by decomposition method. Phys. Scr. **75**, 53–61 (2007)
3. Khan, Y., Diblík, J., Faraz, N., Šmarda, Z.: An efficient new perturbative Laplace method for space-time fractional telegraph equations. Adv. Differ. Equ. **2012** (2012). (Article number 204)
4. Podlubny, I.: Fractional Differential Equations. Academic Press, New York (1999)
5. Metzler, R., Klafter, J.: The random walk's guide to anomalous diffusion: a fractional dynamics approach. Phys. Rep. **339**(1), 1–77 (2000)
6. Zaslavsky, G.M.: Chaos, fractional kinetics, and anomalous transport. Phys. Rep. **371**(6), 461–580 (2002)
7. Meerschaert, M.M., Tadjeran, C.: Finite difference approximations for fractional advection–dispersion flow equations. J. Comp. Appl. Math. **172**, 65–77 (2004)
8. Liu, F., Anh, V., Turner, I.: Numerical solution of the space Fokker-Planck equation. J. Comput. Appl. Math. **166**, 209–219 (2004)
9. Yang, Q., Liu, F., Turner, I.: Numerical methods for fractional partial differential equations with Riesz space fractional derivatives. Appl. Math. Model. **34**, 200–218 (2010)
10. Saichev, A.I., Zaslavsky, G.M.: Fractional kinetic equations: solutions and applications. Chaos **7**(4), 753–764 (1997)
11. Ciesielski, M., Leszczynski, J.: Numerical solutions of a boundary value problem for the anomalous diffusion equation with the Riesz fractional derivative. In: Proceedings of the 16th International Conference on Computer Methods in Mechanics Czestochowa, Poland (2005)
12. Shen, S., Liu, F., Anh, V., Turner, I.: The fundamental solution and numerical solution of the Riesz fractional advection–dispersion equation. IMA J. Appl. Math. **73**(6), 850–872 (2008)
13. Risken, H.: The Fokker-Planck Equation: Methods of solution and Applications. Springer, Berlin (1989)
14. So, F., Liu, K.L.: A study of the subdiffusive fractional Fokker-Planck equation of bistable systems. Phys. A **331**(3–4), 378–390 (2004)
15. Saha Ray, S., Gupta, A.K.: A two-dimensional Haar wavelet approach for the numerical simulations of time and space fractional Fokker-Planck equations in modelling of anomalous diffusion systems. J. Math. Chem. **52**(8), 2277–2293 (2014)
16. Chen, S., Liu, F., Zhuang, P., Anh, V.: Finite difference approximations for the fractional Fokker-Planck equation. Appl. Math. Model. **33**, 256–273 (2009)
17. Zhuang, P., Liu, F., Turner, I., Anh, V.: Numerical treatment for the fractional Fokker-Plank equation. ANZIAM J. **48**, 759–774 (2007)
18. Odibat, Z., Momani, S.: Numerical solution of Fokker-Planck equation with space- and time-fractional derivatives. Phys. Lett. A **369**, 349–358 (2007)
19. Vanani, S.K., Aminataei, A.: A numerical algorithm for the space and time fractional Fokker-Planck equation. Int. J. Numer. Meth. Heat Fluid Flow **22**(8), 1037–1052 (2012)

20. Yildirm, A.: Analytical approach to Fokker-Planck equation with space- and time-fractional derivatives by means of the homotopy perturbation method. J. King Saud Univ. (Science) **22**, 257–264 (2010)
21. Wazwaz, A.M.: Partial Differential Equations and Solitary Waves Theory. Springer, Berlin, Heidelberg (2009)
22. Dodd, R.K., Eilbeck, J.C., Gibbon, J.D., Morris, H.C.: Solitons and Nonlinear Wave Solutions. Academic, London (1982)
23. Debnath, L.: Nonlinear Partial Differential Equations for Scientists and Engineers. Birkhäuser, Boston (2005)
24. Newell, A.C.: Nonlinear Optics. Addition-Wesley, New York (1992)
25. Saha Ray, S.: Numerical solutions and solitary wave solutions of fractional KDV equations using modified fractional reduced differential transform method. Comput. Math. Math. Phys. **53**(12), 1870–1881 (2013)
26. Alfimov, G., Pierantozzi, T., Vázquez, L.: Numerical study of a fractional sine-Gordon equation. In: Workshop Preprints/Proceedings of Fractional Differentiation and Its Applications, FDA 2004, pp. 153–162 (2004)
27. Ivanchenko, YuM, Soboleva, T.K.: Nonlocal interaction in Josephson junctions. Phys. Lett. A **147**, 65–69 (1990)
28. Gurevich, A.: Nonlocal Josephson electrodynamics and pinning in superconductors. Phys. Rev. B. **46**, 3187–3190 (1992)
29. Barone, A., Paterno, G.: Physics and applications of the Josephson effect. Wiley, New York (1982)
30. Aliev, Y.M., Silin, V.P.: Travelling 4π-kink in nonlocal Josephson electrodynamics. Phys. Lett A, **177**(3), 259–262 (1993)
31. Aliev, Y.M., Ovchinnikov, K.N., Silin V.P., Uryupin, S.A. Perturbations of stationary solutions in a nonlocal model of a josephson junction. J. Exp. Theor. Phys., **80**(551) (1995)
32. Alfimov, G.L., Silin, V.P.: On small perturbations of stationary states in a nonlinear nonlocal model of a Josephson junction. Phys. Lett. A **198**(2), 105–112 (1995)
33. Alfimov, G.L., Popkov, A.F.: Magnetic vortices in a distributed Josephson junction with electrodes of finite thickness. Phys. Rev. B: Condens. Matter **52**(6), 4503–4510 (1995)
34. Mintz, R.G., Snapiro, I.B.: Dynamics of Josephson pancakes in layered superconductors. Phys. Rev. B: Condens. Matter **49**(9), 6188–6192 (1994)
35. Cunha, M.D., Konotop, V.V., Vázquez, L.: Small-amplitude solitons in a nonlocal sine-Gordon model. Phys. Lett. A **221**(5), 317–322 (1996)
36. Vázquez, L., Evans, W.A., Rickayzen, G.: Numerical investigation of a non-local sine-Gordon model. Phys. Lett. A **189**(6), 454–459 (1994)
37. Wu, G., Baleanu, D., Deng, Z., Zeng, S.: Lattice fractional diffusion equation in terms of a Riesz-Caputo difference. Physica A-Stat. Mech. Appl. **438**, 335–339 (2015)
38. Rabei, E.M., Rawashdeh, I.M., Muslih, S., Baleanu, D.: Hamilton-Jacobi formulation for systems in terms of Riesz's fractional derivatives. Int. J. Theor. Phys. **50**(5), 1569–1576 (2011)
39. Fahd, J., Thabet, A., Baleanu, D.: On Riesz-caputo formulation for sequential fractional variational principles. Abstr. Appl, Anal. **2012**, 1–15 (2012). (Article Number: 890396)
40. Magin, R.L., Abdullah, O., Baleanu, D., Zhou, X.J.: Anomalous diffusion expressed through fractional order differential operators in the Bloch-Torrey equation. J. Magn. Reson. **190**(2), 255–270 (2008)
41. Meerschaert, M.M., Tadjeran, C.: Finite difference approximations for two-sided space-fractional partial differential equations. Appl. Numer. Math. **56**, 80–90 (2006)
42. Yang, Q., Liu, F., Turner, I.: Computationally efficient numerical methods for time- and space-fractional Fokker-Planck equations. Phys. Scr. **2009**, T136 (2009)
43. Çelik, C., Duman, M.: Crank–Nicolson method for the fractional diffusion equation with the Riesz fractional derivative. J. Comput. Phys. **231**, 1743–1750 (2012)
44. Debnath, L.: Integral Transforms and Their Applications. CRC Press, Boca Raton (1995)

45. Samko, S.G., Kilbas, A.A., Marichev, O.I.: Fractional Integrals and Derivatives: Theory and Applications. Taylor and Francis, London (1993)
46. Saha Ray, S.: Fractional Calculus with Applications for Nuclear Reactor Dynamics. CRC Press, Taylor and Francis Group, Boca Raton, New York (2015)
47. Tarasov, V.E.: Fractional dynamics: applications of fractional calculus to dynamics of particles, fields and media. Springer, Berlin, Heidelberg, New York (2011)
48. Herrmann, R.: Fractional Calculus: An Introduction for Physicists. World Scientific, Singapore (2011)
49. Gorenflo, R., Mainardi, F.: Random walk models for space-fractional diffusion processes. Fractional Calculus Appl. Anal. **1**(2), 167–191 (1998)
50. Saha Ray, S.: Numerical Analysis with Algorithms and Programming. CRC Press, Taylor and Francis Group, Boca Raton, New York (2016)
51. Smith, G.D.: Numerical Solution of Partial Differential Equations: Finite Difference Methods. Oxford University Press Inc., New York, USA (1985)
52. Adomian, G.: Solving Frontier Problems of Physics: The Decomposition Method. Kluwer Academic Publishers, Boston (1994)
53. Khan, Y., Taghipour, R., Falahian, M., Nikkar, A.: A new approach to modified regularized long wave equation. Neural Comput. Appl. **23**, 1335–1341
54. Jafari, H., Sayevand, K., Khan, Y., Nazari, M.: Davey-Stewartson equation with fractional coordinate derivatives. Sci World J **2013**, 8 pp (2013). (Article ID 941645)
55. Kaya, D.: A numerical solution of the Sine-Gordon equation using the modified decomposition method. Appl. Math. Comp. **143**, 309–317 (2003)
56. Wei, G.W.: Discrete singular convolution for the sine-Gordon equation. Physica D **137**, 247–259 (2000)
57. Batiha, B., Noorani, M.S.M., Hashim, I.: Numerical solution of sine-Gordon equation by variational iteration method. Phys. Lett. A **370**, 437–440 (2007)
58. Liao, S.: The proposed homotopy analysis techniques for the solution of nonlinear problems. Ph.D. Thesis, Shanghai Jiao Tong University, Shanghai (1992) (in English)